University of Alberta
Department of Civil Engineering

Structural Engineering Report No. 68

Strength Variability of Bonded Prestressed Concrete Beams

by

D.K. Kikuchi

S.A. Mirza

and

J.G. MacGregor

August 1978

ABSTRACT

The present safety theory for concrete structures is based on reducing the probability of failure to an acceptable value by the use of load and resistance factors. The purpose of this study was to obtain populations of the ratio of theoretical ultimate flexural moment to the ACI design strength for bonded prestressed concrete beams using the Monte Carlo technique. The results of this study will be used in the future to develop understrength factors for prestressed concrete beams in flexure.

Probability models for concrete strength, reinforcing steel strength, and cross section dimensions were obtained from papers on this subject. The probability models for prestressing steel and prestressing losses were developed in this study. Concrete properties, prestressing steel properties, losses, and dimensions of the cross section were varied in this study to examine the effect on the variability of the strength ratios. The type of prestressing strand, the depth of the beam, and the reinforcement index, ω_p, were also varied to see what effect they had on the strength ratios. The effects of construction quality, conventional reinforcing steel, and prestressing losses were also studied.

TABLE OF CONTENTS

LIST OF TABLES

List of Tables (Continued)

LIST OF FIGURES

List of Figures, Continued

CHAPTER I

INTRODUCTION

1.1 General

The present safety theory for concrete structures is based on reducing the probability of failure to an acceptable value by the use of load and resistance factors. An understrength or resistance factor, ϕ, is applied to the strengths and an overload factor, λ, is applied to the loads. The development of an understrength factor requires that the distribution of ultimate strengths be calculated and compared with the strength that would be computed by the designer. This is described in more detail in Section 2.2.

This study is concerned with the calculation of ultimate moment for bonded prestressed concrete beams in flexure. The results are expressed in the form of the ratio of theoretical ultimate strength to the ACI design strength. It is hoped that these results can be used to develop understrength factors for prestressed concrete beams in flexure.

A large population of ultimate strength ratios was obtained for each beam studied through the use of computers and the method of random sampling, also called the Monte

Carlo technique. This technique requires that the probability distribution of every variable affecting the strength be known. Using these probability distributions, random values are generated for each variable using a random number generating subroutine. These values are used in the appropriate equations and a moment-curvature curve is generated. The maximum moment from this curve is determined and taken to be the ultimate moment. When this random sampling procedure is repeated a large number of times, a representative population of ultimate strengths is obtained.

1.2 Scope

Both pretensioned and post-tensioned prestressed concrete beams were studied. The beams were either rectangular beams or T-beams. Two types of prestressing strand were used—stress relieved strand and stabilized, or low relaxation, strand.

Only beams with straight, bonded strand were studied. The beams were all assumed to be simply supported and the section of maximum positive moment was studied.

The overall depth of the beams and the amount of steel was varied. A sensitivity study into the effect of each variable on section strength was conducted. The effects of construction quality, reinforcing steel, and prestressing losses were also investigated.

It was attempted to study practical beams that

are used in prestressed construction. In view of this, many of the beams studied were taken from the *PCI Design Handbook* (1971).

CHAPTER II

LITERATURE REVIEW

A literature review was conducted into flexural theory, safety theory, direct calculation of probability of failure of structural members, and the Monte Carlo technique. Because of the extensive literature in these fields, only a few representative papers will be discussed.

2.1 Flexural Theory

Warwaruk (1957) used a semi-empirical analysis in determining the ultimate strength of prestressed concrete beams. The following assumptions were made in that analysis:

1. Conditions of statics are valid.

2. Concrete fails by crushing at an ultimate strain, ε_u.

3. The strain in the steel can be related to the concrete strain at the extreme fiber in compression using a strain compatibility factor F and the depth to the neutral axis at ultimate, $k_u d$. This compatibility factor is required because strains may not be linearly distributed in the tension zone due to cracking and loss of bond of the

steel to the concrete in this zone. The variation of $F\varepsilon_u$ is mainly due to concentration of the strain near the cracks in bonded beams and to the lack of bond in unbonded beams. If the ultimate steel stress is in the elastic range of the stress-strain curve, variations in $F\varepsilon_u$ can cause large changes in resisting moment. In the inelastic range, however, the value of $F\varepsilon_u$ does not affect the resisting moment significantly.

4. The effective stress of the concrete in the compression zone, f_{cu}, is known. The actual distribution of stress is probably quite similar to the stress-strain curve of cylinders in compression. This distribution was approximated by an average or effective stress. A relationship between effective stress and compressive cylinder strength, f'_c, was found.

5. The ratio, k_2, of the depth to the resultant compressive force in concrete to the depth to the neutral axis was assumed to be equal to 0.42. This value is midway between the extremes of 0.5 and 0.33 for rectangular and triangular stress distributions, respectively. The value of k_2 does not affect the calculated ultimate moment significantly.

6. The stress-strain curve for the prestressing steel is known.

7. No tension is resisted by the concrete. Some tension is, in fact, resisted by the concrete but this ten-

sion force is usually quite small and, at ultimate moment, is insignificant compared to the other forces.

From strain compatibility and equilibrium, the following equations were derived:

$$\varepsilon_{su} = F\varepsilon_u \frac{(1-k_u)}{k_u} + \varepsilon_{se} + \varepsilon_{ce} \qquad (2.1)$$

$$k_u = \frac{\rho_p f_{su}}{f_{cu}} \qquad (2.2)$$

$$M_u = A_{sp} f_{su} d(1 - k_2 k_u) \qquad (2.3)$$

where:

ε_{su} = prestressing steel strain at ultimate moment;

ε_{se} = effective prestrain in steel after losses;

ε_{ce} = the compressive strain in the concrete due to the prestressing force.

If the ratio of prestressed reinforcement ρ_p, f_{cu}, ε_{se}, and the stress-strain curve for reinforcement are known, and $F\varepsilon_u$ is known or assumed, the first two equations can be solved. Once the steel stress at ultimate moment, f_{su}, is known, Equation 2.3 can be used to solve for the ultimate moment. Therefore the calculation of ultimate moment reduces to the determination of the steel stress at ultimate moment. Warwaruk, Sozen, and Siess (1962) suggest that the steel stress can be determined using trial and error, graphical, or algebraic means.

Rüsch (1960) studied the effects of loading rate on the stress-strain curves for concentric compression in concrete. On the basis of a series of such curves, he proposed a stress block for the compression zone in flexure.

Perhaps the most important thing suggested by Rüsch was the definition of failure of a beam in flexure in terms of $dM/d\varepsilon_{cmax} = 0$. That is, there is a maximum point in the curve of resisting moment versus strain in the extreme concrete fiber that corresponds to the ultimate moment capacity of that section.

From this concept, Rüsch also showed that ε_{cu}, the strain in the extreme fiber in compression at ultimate moment, is not a constant quantity for all cross sections but dependent on the shape of the cross section as well as on the position of the neutral axis. For example, the value of ε_{cu} for a T-beam is generally less than that for a rectangular beam and much less than that for a triangular beam.

The suggestion that the strain at ultimate moment varied according to concrete strength, rate of loading, position of neutral axis, and shape of cross section was a departure from previous ultimate strength design theories which assumed a strain at ultimate moment that was constant, or dependent only on concrete strength.

2.2 Safety Theory

MacGregor (1976) reviewed the reasons for re-

quiring safety factors, the techniques for establishing safety provisions, and the derivation of resistance factors (ϕ) and load factors (λ).

Safety factors are required in structural design for three reasons:

1. The strengths of materials or elements may be less than expected due to variability in strengths, rate of loading effects, or the reduction in strength due to *in-situ* effects. Also, the area of the reinforcing bars, the size of the member, or the depth to the steel may be less than what the designer assumes them to be.

2. There may be an overloading of the structure due to variations in load. Both dead and live loads may be more in the structure than was assumed in the design. Actual stresses may be different from the stresses obtained from analysis due to inaccurate assumptions or modelling errors.

3. The result of a failure could be costly not only in terms of repair or replacement but also in terms of the consequences of the failure including the loss of human lives.

One technique for establishing safety provisions is to limit the maximum probability of failure to an acceptable value. The probability of failure is the probability that the loads (U) exceed the strengths (R), that is, the probability that $(R - U) < 0$ or:

$$P_f = P[(R-U) < 0.0] \tag{2.4}$$

A distribution curve for the function Y = R - U is plotted in Figure 2.1. The probability of failure can be represented by the area under the curve in this figure. The probability of failure can also be expressed in terms of the number of standard deviations, $\beta\sigma_Y$, that the mean, $\overline{Y}$, is above zero. The term β is referred to as the safety index since, if the type of distribution is known, β is a measure of the probability of failure.

After some manipulation of Equation 2.4, the following equation is obtained (Cornell, 1969; Lind, 1971; summarized in MacGregor, 1976):

$$R\gamma_R[e^{-\beta\alpha V_R}] \geq U\gamma_u[e^{\beta\alpha V_u}] \tag{2.5}$$

This equation can be rewritten as:

$$\phi R \geq U\lambda \tag{2.6}$$

where:

$$\phi = \gamma_R e^{-\beta\alpha V_R} \tag{2.7}$$

$$\lambda = \gamma_u e^{\beta\alpha V_u} \tag{2.8}$$

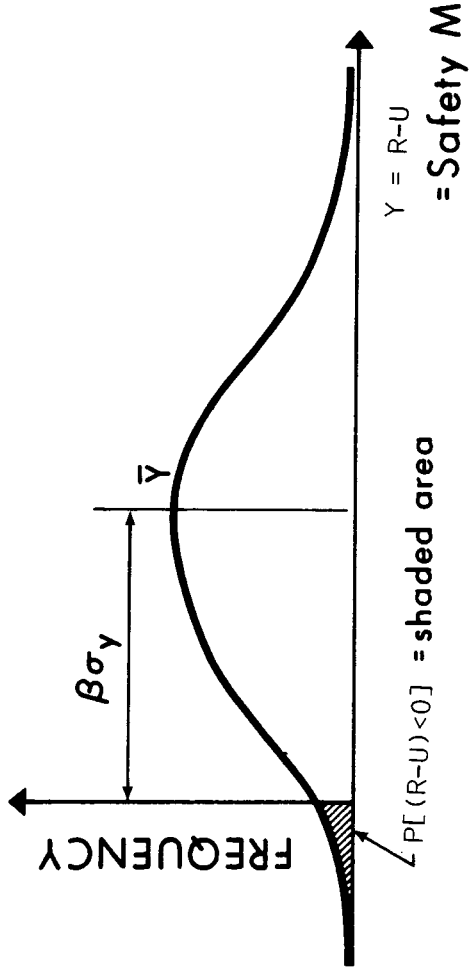

Figure 2.1 Definition of Probability of Failure and Safety Index, β

and:

ϕ = understrength factor;

λ = overload factor;

γ_R = ratio of actual mean strength to strength computed using the code procedures;

γ_u = ratio of actual mean load to the loads specified in the building code;

β = safety index, taken equal to:

3.5 for ductile structures with normal consequences of failure, and

4.0 for severe consequences of failure or brittle failures;

α = a separation factor taken equal to 0.75;

V_R = the coefficient of variation of the strength or resistance;

V_u = the coefficient of variation of the loads.

The values of β were chosen to obtain sufficiently low probabilities of failure, 10^{-4} in 30 years for ductile structures and 10^{-5} in 30 years for brittle structures.

The results from the present study will be values of γ_R and V_R which can be used in Equation 2.7 to calculate the understrength or ϕ factor for prestressed concrete beams.

2.3 Direct Calculation of Probability of Failure of Structural Members

Chandrasekar and Dayaratnam (1975) studied the probability of failure of prestressed concrete beams which were designed by the Indian Standards (IS) Code and the ACI Code. The strengths of materials were generated as random variables, the only restriction being that code specifications had to be met. The loads were treated as deterministic in one case and as having a probability distribution in the second. The probability of failure was then calculated using equations.

The probability of failure of the beams decreased as the amount of steel was increased. Varying the strength of concrete did not influence the probability of failure significantly because the beams were underreinforced. Very low probabilities of failure were obtained for the codes used; of the order of 10^{-14} for deterministic loads and of the order of 10^{-11} for probabilistic loads.

Ellingwood and Ang (1974) also used a probabilistic approach to failure. The level of risk was evaluated from an analysis of the uncertainties in the design. Uncertainties, Ω, in the variables are functions of the basic variabilities, δ, and the prediction errors, Δ, as given by $\Omega^2 = \delta^2 + \Delta^2$. The mean value and the basic variability (δ) for each variable were estimated from available data. The basic variabilities (δ) could exist even if the designer and fabricator took all due care.

The prediction error (Δ) accounts for inaccuracies in estimating the mean. Ellingwood attributes these prediction errors to modelling errors, insufficient information, and inaccurate calculations in design. If sufficient data on the variables are available, Δ can be set equal to the coefficient of variation. Otherwise, it may have to be estimated by estimating a range of values for the mean and then assuming a distribution over this range. In other cases, it may be necessary to use only judgment and past experience to choose Δ.

The uncertainties in f_y, f_c, b, d, and A_s were found using the basic variability and the prediction error for each variable. The uncertainty in the limiting strain, ε_{cu}, was also found since this variable was required to calculate the uncertainty in the balanced reinforcement ratio ρ_b. The uncertainties in the coefficients defining the concrete compressive stress distribution were also found.

The various uncertainties did not contribute equally to the uncertainty of M_T (the mean flexural capacity of a beam failing in tension). For lightly reinforced sections, the uncertainties of f_y, A_s, and d contributed greatly towards the uncertainty of M_T. As the amount of reinforcement increased, f_c, b, and the stress block parameters became more important which indicates that the moment at tension failure is more affected by crushing of the concrete for high amounts of reinforcement. Concrete

quality control (variability of f_c) and the mean value of the steel ratio were found to have little influence on the uncertainty of M_T. The uncertainty of M_C, the flexural capacity in compression, was higher than the uncertainty of M_T. Concrete quality control had more influence on the flexural strength for compression failures than for tension failures.

This probability approach was used to obtain the uncertainty in shear capacity. The uncertainties in shear capacity were considerably larger than those in flexure; however, the shear uncertainties were not affected by concrete quality control. The uncertainty of dead and live loads were also investigated.

The level of safety in the *ACI Building Code* (1971a) was evaluated using this risk analysis procedure. It was found that under the ACI restrictions, there is a probability of compressive failure as high as 25 percent for a steel ratio at the limit of 75 percent of the nominal balanced steel ratio. Also, the probability of shear failures (which are more dangerous than flexural failures because they give less warning) was higher than the probability of flexural failure for a wide range of the mean value of the steel ratio. The authors suggest lowering the reinforcement ratio limit to 50 percent of the mean balanced steel ratio to decrease the likelihood of a compression failure, and reducing the capacity reduction factor, ϕ, for shear to about 0.75 from its present value of 0.85,

to ensure that the risk of a shear failure is less than the risk of a flexural failure.

2.4 Monte Carlo Technique

The concept that strength is dependent on factors that are multivalued was used to determine a factor of safety for timber structures (Wood, 1958). Wood used frequency distributions to describe these factors. Although he called his procedure the method of random products, it is the same as the Monte Carlo technique. Wood stated that:

> The method of random products consists of taking a random value from the frequency distribution that represents each factor and multiplying these random values together to obtain a random product.

Warner and Kabaila (1968) described the concept of using a Monte Carlo technique in conjunction with high speed computers to evaluate structural safety. Their technique consisted of three steps.

1. Random values for the material properties and geometric parameters were generated in accordance with the density functions of these properties and parameters.

2. The structural response corresponding to these random values was calculated using a strength prediction equation.

3. Steps 1 and 2 were repeated until a large population of structural responses was obtained. From this

population, it would be possible to estimate the probability of the response falling below a particular value.

Warner and Kabaila present the variability of a short reinforced concrete column as an example. The results agree very well with the closed form solution.

The authors point out that very often only a small part of the distribution is of interest to the investigator. A few selective sampling techniques are suggested so that the desired information is obtained in a minimum number of simulations.

Allen (1970) has studied the variability of flexural failures for reinforced concrete beams reinforced in tension only. Allen's approach was very similar to that used in this study. He derived prediction equations for the ultimate moment and ductility ratio (ratio of curvature at ultimate to curvature at yield) for beams developing tension and compression failures. Probability distributions for the parameters involved in computing ultimate moment were obtained. A Monte Carlo analysis was then used to compute the probability distributions of the ultimate moment and ductility ratio.

The prediction equations were derived using the equivalent rectangular stress block for the compression zone and the assumption that plane sections remain plane. The concrete was assumed to have no tensile strength. The limiting strain in concrete and other parameters defining the concrete strength and the shape of the stress

block were determined from tests.

The prediction equations were found to predict the ultimate moment very accurately. The mean of the ratio of the ultimate test strength to the ultimate predicted strength was only 1.01 for tension failures and 1.00 for compression failures. The coefficient of variation of this ratio was 3.1 percent for tension failures and 5.7 percent for compression failures. Most of this dispersion could be attributed to variation of the actual test beam parameters from the measured values.

The effect of rate of loading on the compressive strength of concrete was taken into account by Allen. He also considered the rate effect in determining the probability model for yield strength for reinforcing steel. A normal distribution was used for yield strength.

Two levels of workmanship—minimum and good—were considered in the distributions for concrete strength and dimensions.

The results for ultimate moment were reported in the form of a ratio of predicted ultimate moment to the ultimate moment calculated using the 1963 ACI Code. The distribution of this ratio was close to being normal.

Allen concluded that there is a significant possibility that a section will have a compression failure even when it is underreinforced according to ACI318-63 due to variations in the concrete strength. This agrees with Ellingwood's observation mentioned earlier. He also

concluded that:

> The average ultimate moment [ratio] is more or less independent of depth to reinforcing, percentage of steel, and workmanship.

However, he found that the variability of the ultimate moment increased for shallow sections (i.e., thin slabs) or for high steel percentages whereas good workmanship decreased the variability. Rate of loading had little effect on the variability of the ultimate moment.

The distribution for ductility ratio was skewed positively. This ratio had a higher variability than did ultimate moment.

CHAPTER III

THEORETICAL BEHAVIOUR OF PRESTRESSED CONCRETE SECTIONS

3.1 Basic Assumptions in Analysis

In order to analyze a prestressed concrete section, several assumptions had to be made. These assumptions were:

1. Plane sections remain plane after loading. That is, the strains in the beam cross section are proportional to the distance from the neutral axis which leads to a linear strain distribution at the cross section.

2. The strain in the reinforcing steel was assumed to be equal to the strain in the concrete at the same point in the beam. In other words, perfect bond was assumed to exist and the strain compatibility factor, F, was equal to 1.0 (see Section 2.1).

3. The strain in the prestressing steel was assumed to be greater than the corresponding concrete strain due to the pretension strain that occurs in the steel before the concrete is bonded to the prestressing strands. Figure 3.1 shows that, relative to the unstressed state, this prestrain

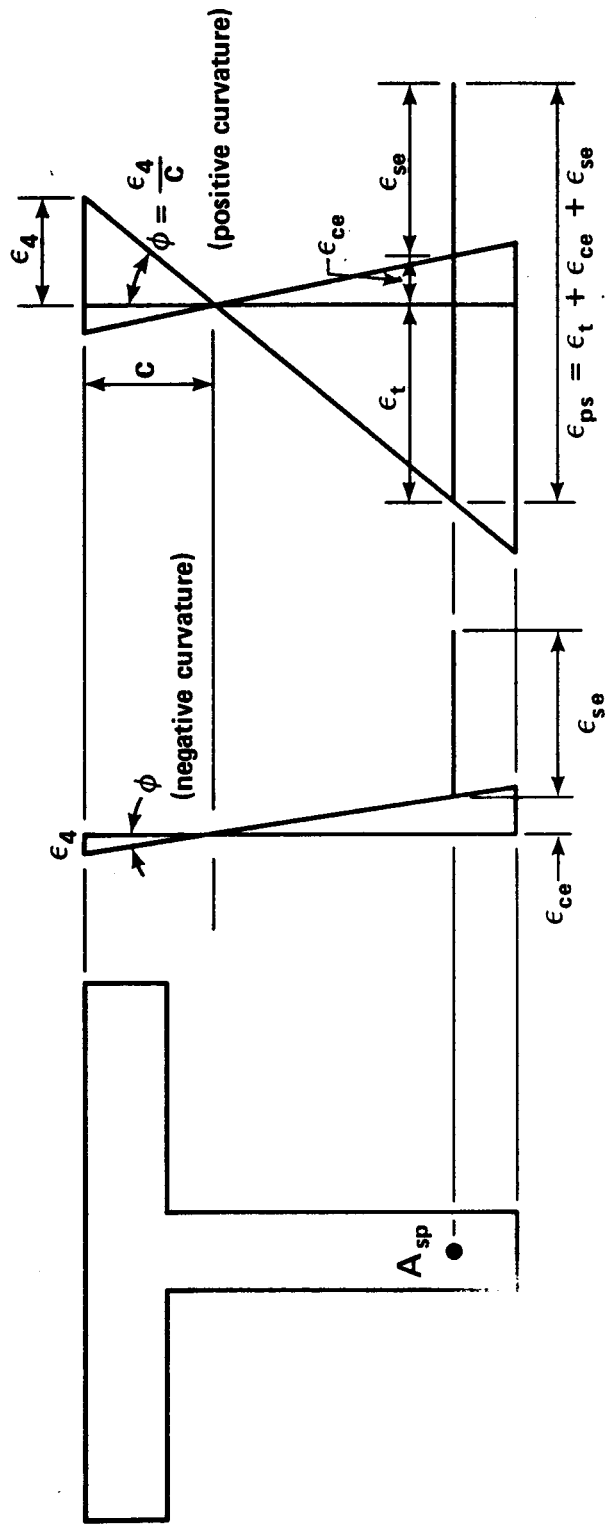

Figure 3.1 Distribution of Strain Assumed in Analysis

is made up of two parts—the effective prestrain in the steel after losses, ε_{se}, and the compressive strain in the concrete due to the prestressing force, ε_{ce}. After bonding occurred, however, any change in strain in the concrete was accompanied by the same change in prestressing steel strain. Hence, once a bond has occurred, this bond was assumed to be perfect.

4. The stress in the concrete could be determined from the strains using a modification of Hognestad's stress-strain curve in compression and an elastic line in tension (see Section 3.2).

5. The stress-strain relationship for the reinforcing steel was assumed to be elastic-plastic.

6. The stress in the prestressing steel was determined from the strains using a stress-strain curve composed of two straight lines and a parabola (see Section 3.4).

7. The forces acting on a cross section must be in equilibrium.

8. The maximum moment capacity of a given cross section corresponds to the maximum point in the moment-curvature diagram for that cross section (Rüsch, 1960).

3.2 Stress-Strain Relationship for Concrete

A variation of Hognestad's (1952) stress-strain curve for concrete was used in the theoretical analysis of

prestressed concrete sections. Hognestad's curve consists of a second order parabola up to a maximum stress of $f''_c = 0.85f'_c$ which occurs at a strain $\varepsilon_0 = 2f''_c/E_c$ where E_c is the initial tangent modulus of elasticity of concrete defined in Section 4.1. Beyond the maximum stress, the stress is assumed to decrease linearly with increasing strain to a value of $0.85f''_c$ at the ultimate strain, ε_u, taken by Hognestad as 0.0038. In this study, the same expression for ε_0 and the same value of ε_u was used. The stress-strain curve used in this study, shown in Figure 3.2, differed from Hognestad's curve only in that the maximum stress was set equal to the *in-situ* strength of concrete, adjusted for the effects of the rate of loading, f_{cstrR}. This particular strength is described more fully in Section 4.1.

The tensile strength of concrete was also considered in this study. The reason for its inclusion was the need for as high a degree of realism as possible in calculating forces and moments.

A linear relationship between tensile stress and strain in concrete was assumed up to the strain at which the concrete cracks, ε_r (see Section 4.1). At tensile strains greater than this cracking strain, the stress was zero as is shown in Figure 3.2. The modulus of elasticity was assumed to be equal in tension and compression.

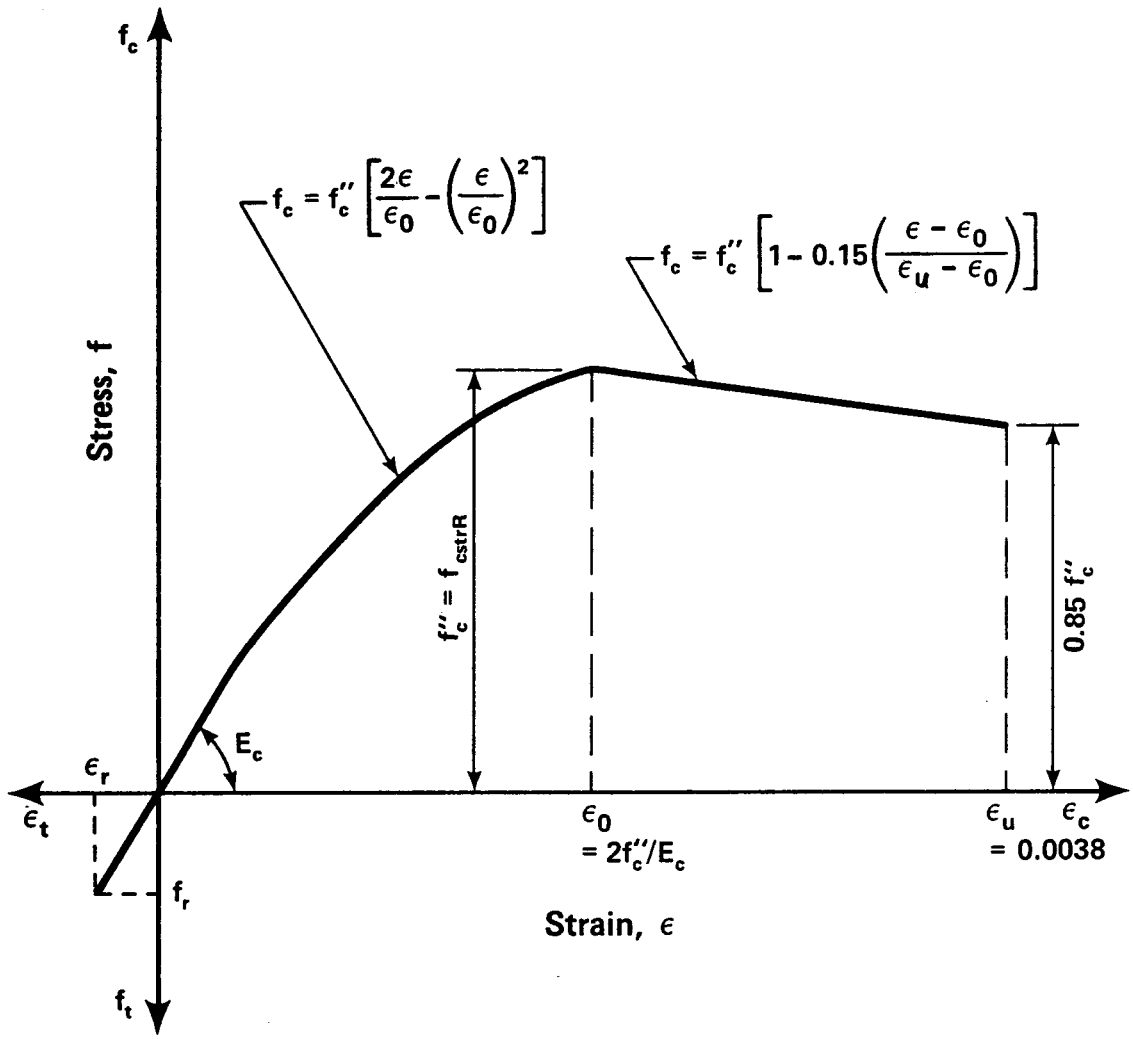

Figure 3.2 Stress-Strain Curve for Concrete

3.3 Stress-Strain Relationship for Reinforcement

The stress-strain relationship for conventional deformed reinforcement was assumed to be elastic for strains less than the yield strain, $\varepsilon_y = f_y/E_s$ where f_y and E_s are the yield strength and the modulus of elasticity, respectively, as defined in Section 4.2. At strains greater than the yield strain, the stress was equated to the yield strength. Because the onset of strain hardening in the reinforcement occurs at strains close to the failure strains of the prestressing tendons, strain hardening should have little effect on the strength and was ignored.

3.4 Stress-Strain Relationship for Prestressing Steel

Two types of prestressing steel strand were considered in this study, stress relieved and stabilized. The main difference between stress relieved and stabilized steel is that the stabilized steel has been further heat treated and subjected to high tension to reduce relaxation losses. As described in Section 4.3, the process of stabilization results in slightly improved stress-strain characteristics. This improvement is reflected in the stress-strain curve for stabilized strand used in this study. The assumed stress-strain curve for stress relieved strand will be described first, followed by a description of how the stress-strain curve for stabilized strand is different.

The stress-strain curve for stress relieved

strand was taken to be linear up to the elastic limit of 70 percent of the ultimate stress. From this point to the stress at 1 percent strain, the curve was defined by a second straight line as shown in Figure 3.3. The average value of the stress at 1 percent strain was found to be 89 percent of the ultimate stress although, as discussed in Section 4.3, it could be as high as 94 percent or as low as 84 percent of the ultimate stress. The part of the curve from 1 percent strain to the failure strain, point C to point D in Figure 3.3, was taken as a parabola. The equations for the three regions are:

Region I ($0 < \varepsilon \leq 0.7f_{pu}/E_{sp}$):

$$\sigma = E_{sp} \cdot \varepsilon \tag{3.1}$$

Region II ($0.7f_{pu}/E_{sp} < \varepsilon \leq 0.01$):

$$\sigma = 0.7f_{pu} + \frac{\left(\sigma_1 - 0.7f_{pu}\right)\left(\varepsilon - \frac{0.7f_{pu}}{E_{sp}}\right)}{\left(0.01 - \frac{0.7f_{pu}}{E_{sp}}\right)} \tag{3.2}$$

Region III ($0.01 < \varepsilon \leq \varepsilon_{up}$):

$$\sigma = \frac{-b + \sqrt{b^2 - 4ac}}{2a} \tag{3.3}$$

where:

$$a = \frac{\alpha}{f_{pu}{}^2}$$

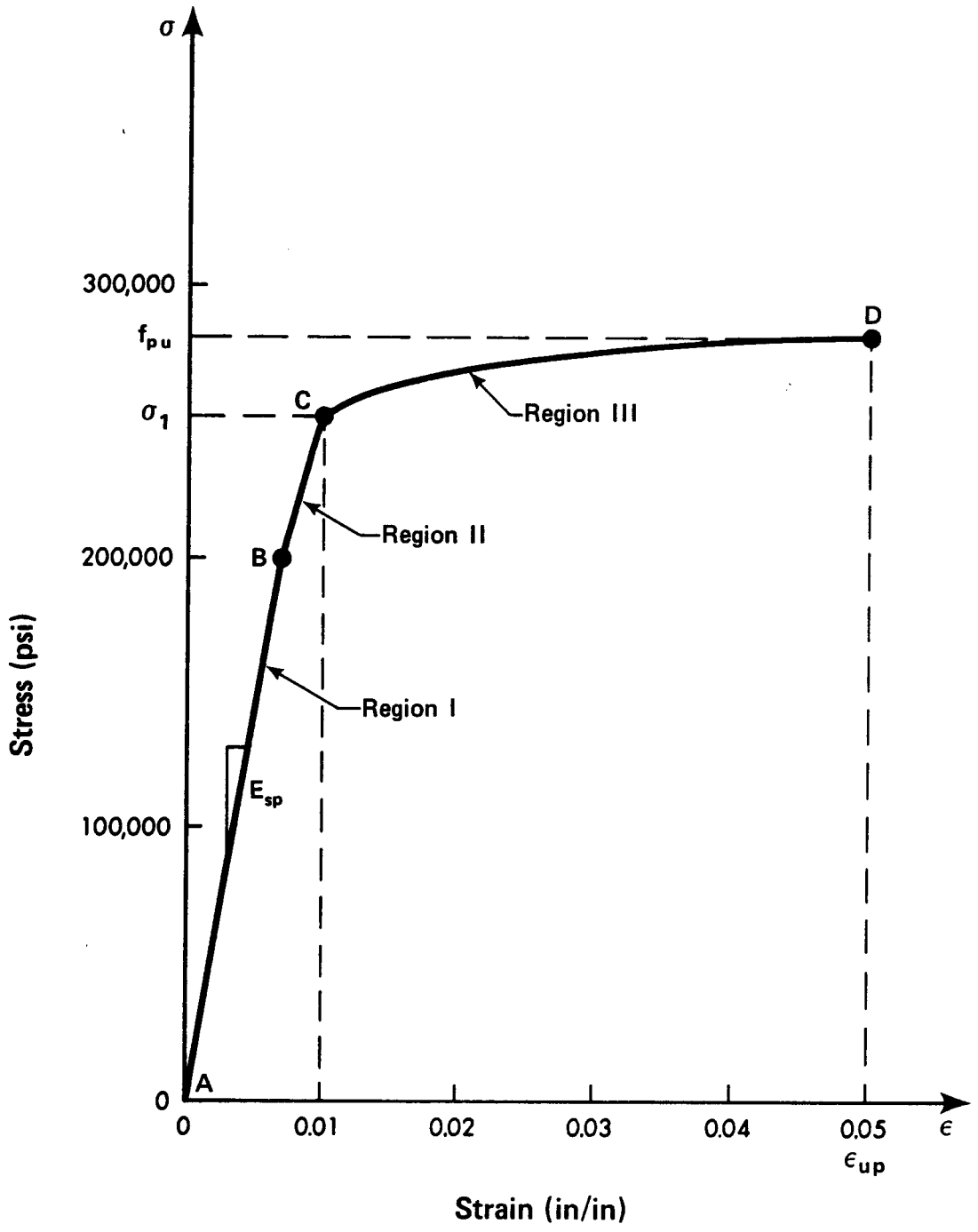

Figure 3.3 Stress-Strain Curve for Prestressing Steel

$$b = \frac{-2\alpha\beta}{f_{pu}}$$

$$c = \alpha\beta^2 + 0.01 - \varepsilon$$

$$\alpha = \frac{\varepsilon_{up} - 0.01}{(1 - \beta)^2}$$

$$\beta = \frac{\sigma_1}{f_{pu}}$$

σ_1 = stress at 1 percent strain

f_{pu} = ultimate tensile strength

ε_{up} = ultimate strain of prestressing steel

E_{sp} = modulus of elasticity of prestressing steel

The parabola used in this study was adapted from a stress-strain curve proposed by Murray and Epstein (1976). In that work, a parabola was used to describe the stress-strain curve between the elastic limit and the ultimate stress:

$$0.7f_{pu} < \sigma < f_{pu}$$

$$\varepsilon = \frac{\sigma}{E_{sp}} + 0.1\left(\frac{\sigma}{f_{pu}} - 0.7\right)^2 \qquad (3.4)$$

Equation 3.4 tended to underestimate the stress at small

strains where the curve started to bend over and reached the ultimate stress at too small a strain. This resulted in a straight, horizontal line from medium strains to the ultimate strain at the level of the ultimate stress. As can be seen in Figure 3.3, using the parabola between points C and D instead of between points B and D seems to overcome this problem. It should also be noted that in Murray's work, the stress was used in the parabola equation to solve for strain. On the other hand, the analysis in this study required that the strain be used to solve for the stress. This involved solving a quadratic equation, as can be seen in Equation 3.3. Since the root required was always the higher one, however, the solution was simplified somewhat.

The stress-strain curve for stabilized strand was assumed to be linear up to 75 percent of the ultimate stress, rather than 70 percent in the case of stress relieved strand. In addition, the stress at 1 percent strain was assumed to be a little higher for stabilized strand, averaging 90 percent of the ultimate stress, with a maximum and minimum of 95 percent and 85 percent, respectively. Thus, Equation 3.1 applies up the yield strain which is now defined as $0.75f_{pu}/E_{sp}$ and Equation 3.2 must be changed for stabilized strand:

Region II ($0.75f_{pu}/E_{sp} < \varepsilon \leq 0.01$):

$$\sigma = 0.75f_{pu} + \frac{\left(\sigma_1 - 0.75f_{pu}\right)\left(\varepsilon - \frac{0.75f_{pu}}{E_{sp}}\right)}{\left(0.01 - \frac{0.75f_{pu}}{E_{sp}}\right)} \qquad (3.5)$$

The term β, defined earlier, takes into account the magnitude of the stress at 1 percent strain in Region III.

Thus, the stress-strain curve for prestressing steel can be described using four parameters:

1. the modulus of elasticity,

2. the ratio of stress at 1 percent strain to ultimate stress,

3. the ultimate stress, and

4. the ultimate strain.

Values for these four terms are presented in Section 4.3 of this report.

3.5 Method for Developing the Moment-Curvature Diagram

The moment-curvature diagram was developed for a beam having the properties generated in each simulation in the Monte Carlo program. The maximum moment from the moment-curvature diagram was assumed to be the ultimate moment capacity of the section and was compared to the ultimate moment computed according to the ACI Building Code (1971a). A typical moment-curvature diagram for prestressed concrete beams is shown in Figure 3.4. Curvature is defined as the ratio of the strain at the extreme concrete fiber to the depth to the neutral axis.

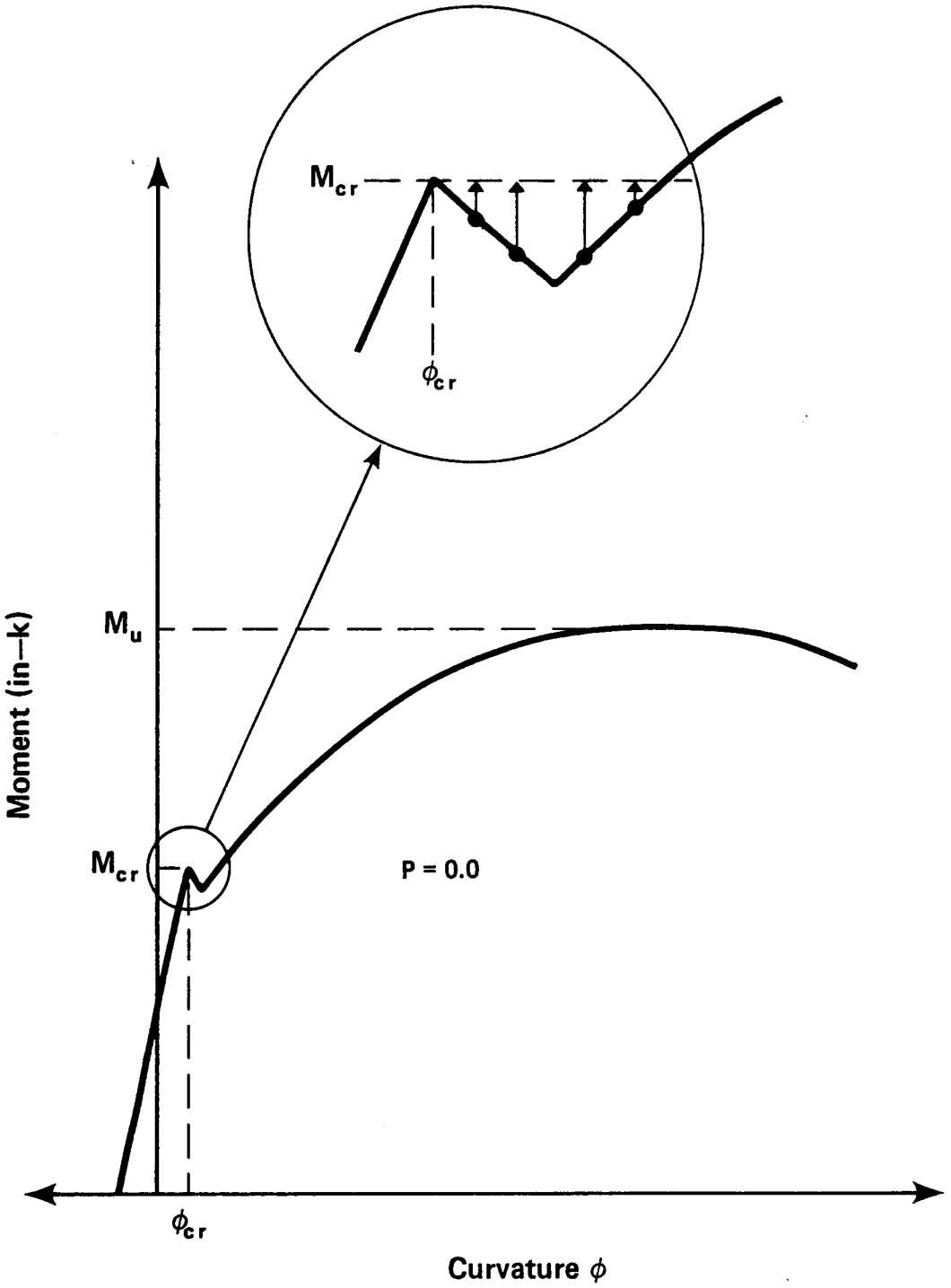

Figure 3.4 Typical Moment-Curvature Diagram for a Prestressed Concrete Beam

The moment-curvature diagram was developed by incrementing curvature. For a particular curvature, the strain at the top of the section was altered using either the Newton-Raphson procedure or a trial and error procedure until the compression and tension forces in the section were essentially equal. These procedures are further described in the balance of this section and in Section 3.6. Once the forces were balanced, the moment was calculated and thus one point on the moment-curvature diagram was determined. The curvature was then incremented and the above procedure of balancing the forces and calculating the moment was repeated. This was continued until the change in moment after an increment in curvature was so slight that for all practical purposes, the ultimate moment had been reached.

Before the calculation of the forces is described, a brief explanation of the notation and sign convention is in order. The basic notation for dimensions, strains, stresses, and forces is shown in Figure 3.5. The strain at the top of the section is ε_4, the strain at the bottom of the flange is ε_3, and the strain at the bottom of the section is ε_1. Compressive strains and forces were taken as positive. A positive moment was taken as counterclockwise as shown in Figure 3.5.

The compressive force in the concrete was calculated by splitting the stress distribution into three parts as shown in Figure 3.6. The area under the parabola could be calculated by integrating the equation for the parabola

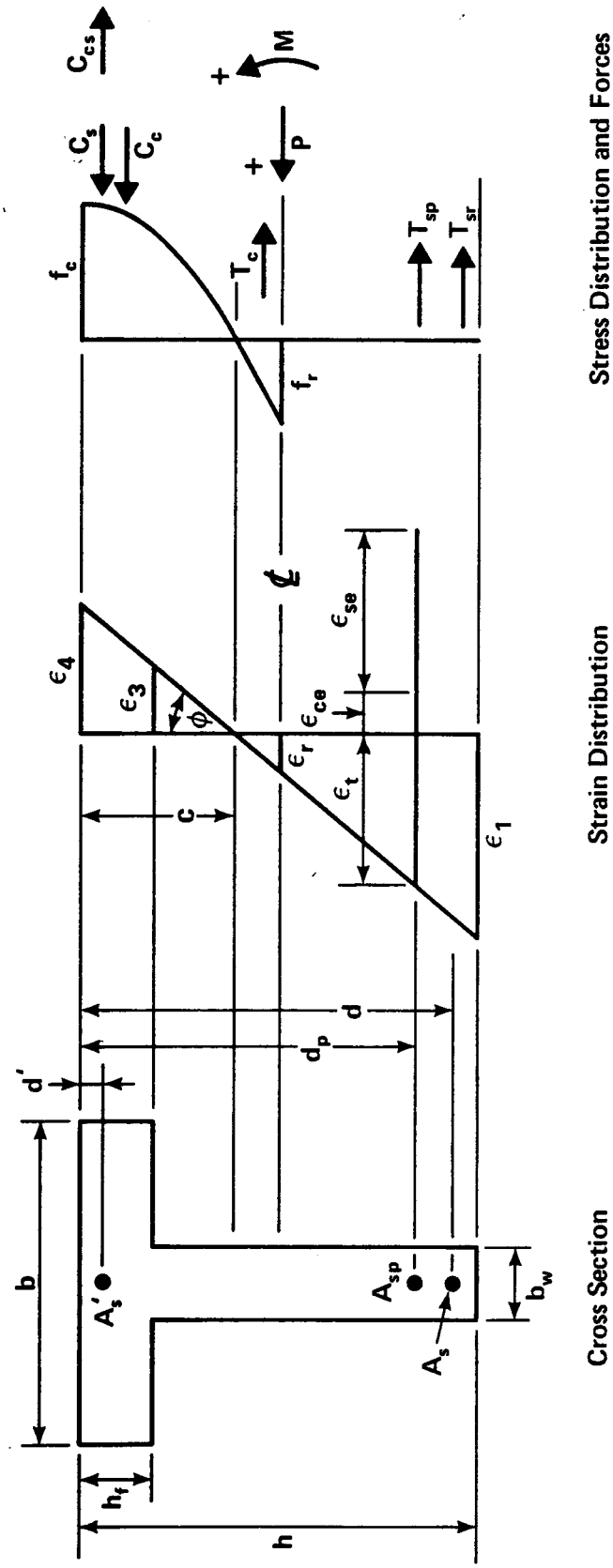

Figure 3.5 Basic Notation

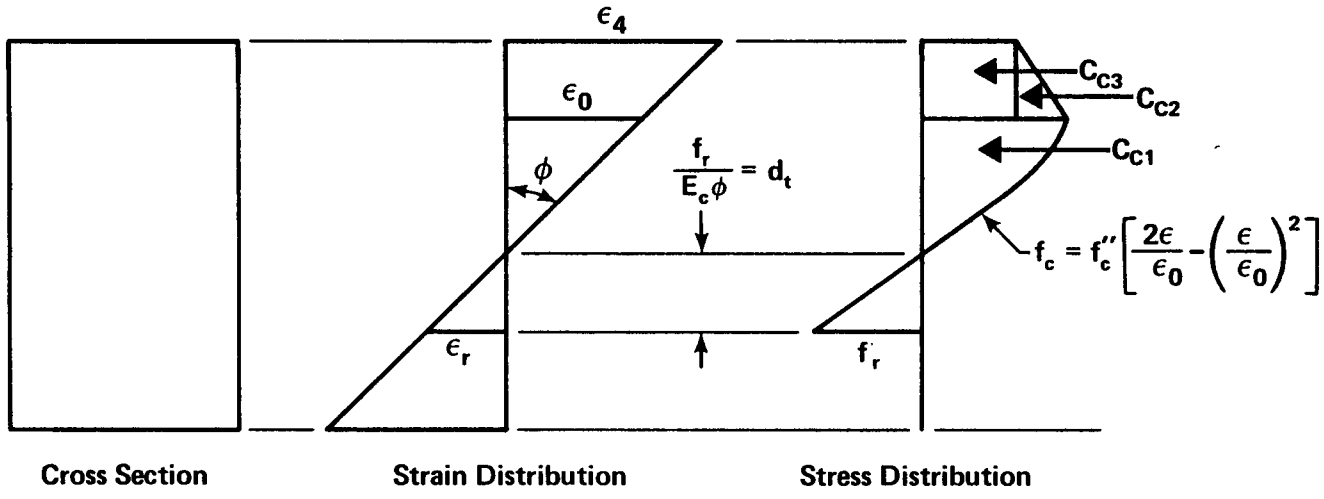

Figure 3.6 Stress Distribution Divided Into Parts

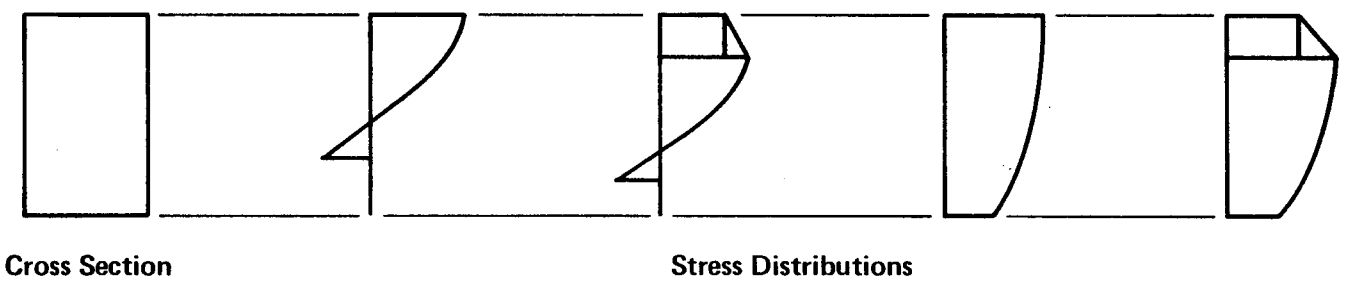

Figure 3.7 Four Basic Cases of Compressive Stress Distribution

as suggested by Gurfinkel and Robinson (1967):

$$\text{Area} = \frac{c}{\varepsilon_4} \int_0^{\varepsilon_4} f''c\left[\frac{2\varepsilon}{\varepsilon_0} - \left(\frac{\varepsilon}{\varepsilon_0}\right)^2\right] d\varepsilon \qquad (3.6)$$

The areas of the triangle and the rectangle could be calculated using simple geometric relationships. These areas are multiplied by the width of concrete that is influenced by this stress distribution to give the force in that part of the compression zone. For a rectangular cross-section, there were four basic cases as shown in Figure 3.7. For a T-section these basic cases had to be adjusted slightly to take into account the area of the flange. There are nine different cases to consider for a T-section. The various cases for rectangular and T-beams and the corresponding equations are summarized in Appendix A. The four cases for the rectangular section are included in the nine cases for the T-section since in a rectangular section, $b = b_w$ and some unnecessary terms drop out in the equations. It should be noted that some of these equations are not very accurate for very low values of ε_4 and ε_3 since these terms are taken to the third or fourth power at times. This inaccuracy did not affect the results of this study, however, since the critical ranges correspond to high values of ε_4.

The tension force in the concrete was calculated by multiplying the area under the triangular stress distribution by the width of the concrete influenced by this stress

distribution. This may be expressed as:

$$T_c = \left(\frac{1}{2} f_r \times \frac{f_r}{E_c \phi}\right) b_w \qquad (3.7)$$

where $\frac{f_r}{E_c \phi}$ is the distance shown in Figure 3.6.

For a given strain distribution, the strain in each reinforcing bar was obtained. The corresponding stress was obtained from the stress-strain curve. This stress, when multiplied by the bar area, gave the steel force.

Similarly, the strain at the level of the prestressing tendons, ε_t, could be determined for a given strain distribution. As explained in Section 3.1 and Figure 3.1, the total strain in the prestressing steel is:

$$\varepsilon_{ps} = \varepsilon_t + \varepsilon_{ce} + \varepsilon_{se} \qquad (3.8)$$

The load gradually reduces the compressive strain in the concrete due to the prestressing force, ε_{ce}, to zero strain before the concrete at the level of the prestressing steel goes into tension.

Once the strain in the prestressing steel was known, the stress was obtained from the stress-strain curve and the force was obtained by multiplying this stress by the tendon area.

Concrete that was displaced by the steel was taken into account by calculating the compressive force that this amount of concrete would have exerted, C_{cs}, and then sub-

tracting it from the compressive force. This displaced concrete was taken into account only when the steel was above the neutral axis.

The total force acting on the section was obtained by summing all of these forces:

$$P = C_c + T_c + T_{sr} + T_{sp} + C_s + C_{cs} \tag{3.9}$$

As explained earlier, tensile forces are negative. These forces should add up to zero since this was a beam and there was no axial force on it. The computer program had a tolerance built into the force balancing procedure so that the sum of forces was close to, but not necessarily equal to, zero.

Once the forces were balanced within tolerance, the moment was calculated by multiplying the forces by their moment arms:

$$M = C_c \cdot y + T_c\left[\frac{h}{2} - \left(c + \frac{2}{3}d_t\right)\right] + T_{sr}\left[\frac{h}{2} - d\right] +$$

$$T_{sp}\left[\frac{h}{2} - d_p\right] + (C_s + C_{cs})\left[\frac{h}{2} - d'\right] \tag{3.10}$$

The expressions for the moment arms for the compressive force in the concrete are given in Appendix A. All the moments were summed about midheight. This introduces a small error since the resultant force, P, acts at the centroid which is not at midheight for T-beams, and should thus con-

tribute to the total moment. However, the moment due to P would not significantly affect the total moment because the tolerance on P was small enough that P was close to zero.

Figure 3.4 shows that a prestressed concrete beam is initially subjected to negative curvature. This is caused by the prestressing force which makes the beam camber upwards before any load is applied. At this stage, the top of the beam is in tension (or at a small compression) and the bottom of the beam is in compression as shown in Figure 3.1(a).

Figure 3.4 also shows that for a small increase in curvature, the moment decreases slightly at the cracking moment, M_{cr}. The cracking moment is the bending moment at which the strain at the bottom of the section reaches the cracking strain. Up until this point, the tension force in the concrete increases as the strain in the concrete increases. As soon as the concrete cracks, however, the tension force in the cracked concrete disappears. As the cracking in the concrete progresses upward, the tension force in the concrete reduces in magnitude and moves toward the neutral axis causing a slight decrease in moment at this point. As the curvature increases, however, this reduction in moment is soon offset by an increase in the moment due to the increase in the reinforcement stress.

The decrease in calculated moments at cracking was found to stop the development of the full moment-curvature diagram in some cases. This problem was overcome

by finding the cracking moment and cracking curvature and then bringing the magnitude of the moment up to the level of the cracking moment if the curvature was greater than the cracking curvature. This is shown graphically in Figure 3.4. In effect, the dip in the curve was eliminated and was replaced by a horizontal line.

The cracking moment and cracking curvature were calculated using a trial and error procedure. The strain at the bottom of the section was assumed equal to the cracking strain and the curvature was incremented until the compression and tension forces were equal within a tolerance.

In a few cases, a second dip in the moment-curvature diagram was observed when the tension block in the concrete extended into the flange of a T-beam.

Generally, the ultimate moment was reached when either the strain in the concrete at the top of the section reached the ultimate strain, ε_u, or the strain in the prestressing steel reached the ultimate strain, ε_{up}. However, in some cases, the maximum moment was found to occur when the strains in the concrete and steel were less than the ultimate strains. The shape of the compressive stress block was partly responsible for this, as illustrated in Figure 3.8 for one particular case. The increase in ϕ and ε_4 results in a change in stress distribution, shown by the dotted lines. As ϕ and ε_4 increase:

1. ε_{ps} increases, resulting in increases in the steel stress, force and moment;

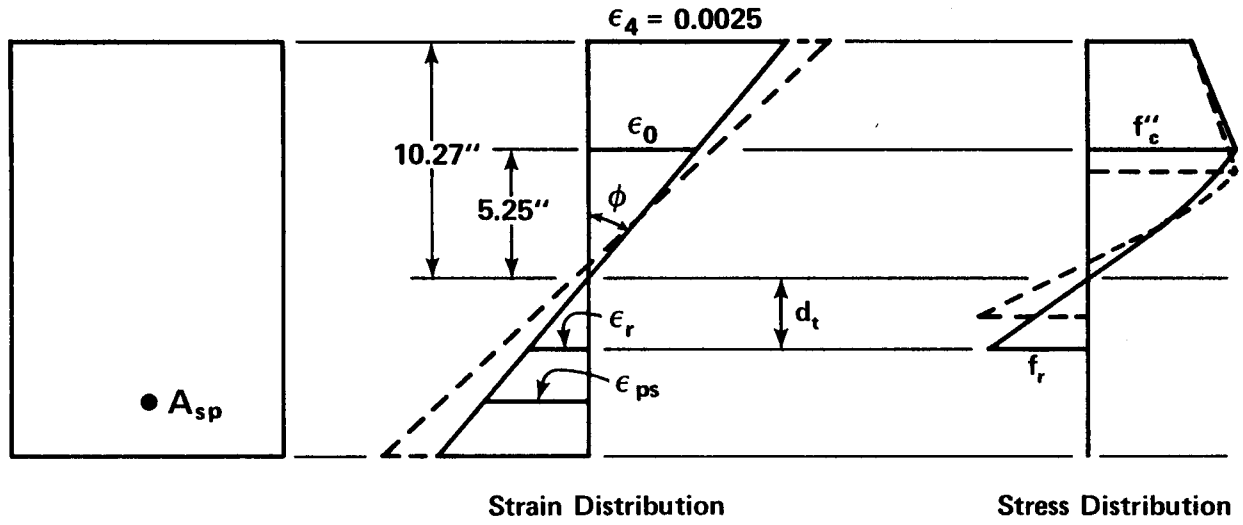

Dotted Lines Indicate Distributions as ϕ and ϵ_4 Increase

Figure 3.8 Strain and Stress Distributions at Ultimate Moment for One Particular Case

2. The tension force in the concrete decreases due to a decrease in d_t. Also, this force gets closer to mid-height, therefore, the moment due to the tension force decreases.

3. The compressive force in the concrete may decrease because the position of ε_0 moves down. There is less contribution from the parabola portion of the compressive block and slightly more from the trapezoidal part. The centroids of the parabola and trapezoid both move down resulting in smaller moment arms and a smaller moment due to the compressive force in the concrete.

If the decrease in the moments of the concrete forces is more than the increase in the moment of the steel force, the total moment will decrease. This beam was investigated at the ultimate moment condition assuming the concrete strain was at the ultimate strain and the moment was found to be less than the moment for the distributions shown in Figure 3.8. Thus, the ultimate moment may be reached before the strains in the concrete and steel reach their so-called ultimate strains.

3.6 Numerical Analysis Techniques

Two techniques were used to determine the strain at the top of the section, ε_4, that would balance the forces. The first technique was the extended Newton-Raphson method. This method was used by Gurfinkel and

Robinson (1967) to determine the strain distribution in a reinforced concrete section that was subjected to combined axial load and bending moment. In this study, the section is not subjected to a longitudinal load so the procedure is simplified somewhat. The Newton-Raphson technique converges on the correct value of ε_4 very quickly. Thus, the computer program used in this study tries to use this method wherever possible. However, this technique does break down in a few cases, as discussed later in this section. When this happens, a trial and error technique is employed.

The Newton-Raphson procedure is used on nonlinear curves. In this case, it is used on the force-top strain ($P - \varepsilon_4$) curve which can have inflection points, as shown in Figure 3.9. There is one $P - \varepsilon_4$ curve for each curvature, ϕ. The upper part of the curve becomes flatter as ε_4 increases (keeping ϕ constant) because the compressive stress in the concrete does not increase as fast as the strain due to the shape of the stress-strain curve for concrete. [See Section 3.2 and Figure 3.10(a).] As ε_4 decreases, the compressive stress and hence the compressive force decreases as well. Eventually, as ε_4 continues to decrease, the concrete cracks in tension and, because the $P - \varepsilon_4$ curve is plotted for a constant value of ϕ, the tension force remains constant while the compressive force continues to decrease as shown in Figure 3.10(b). Depending on the magnitude of the steel force, the resultant force, P,

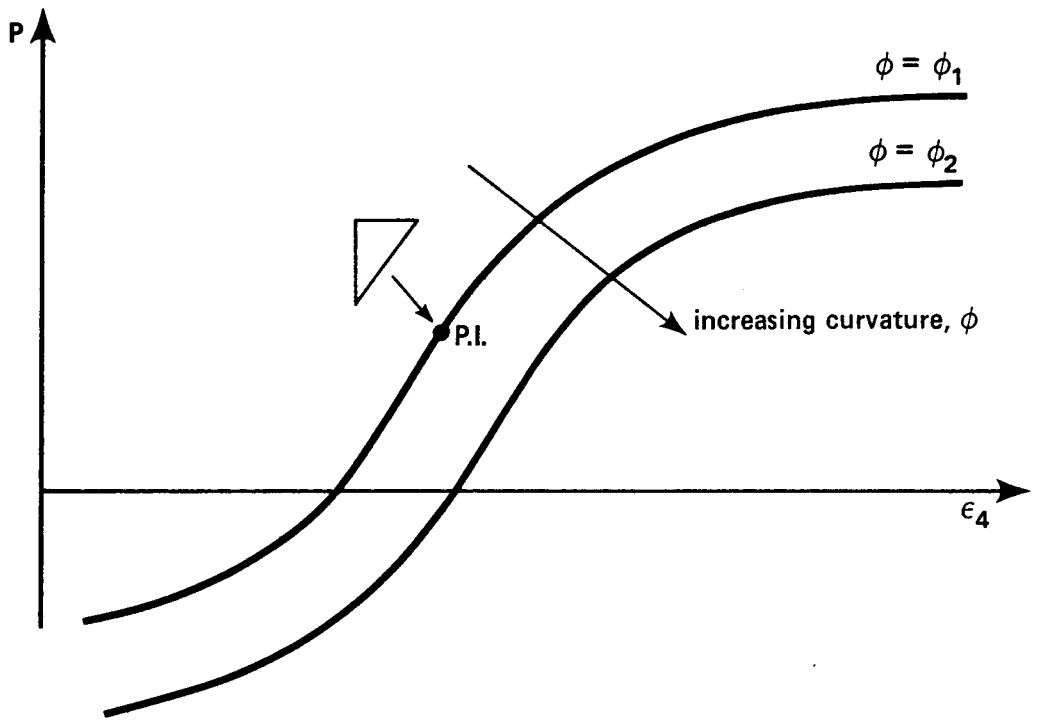

Figure 3.9 Typical P - ϵ_4 - ϕ Curves

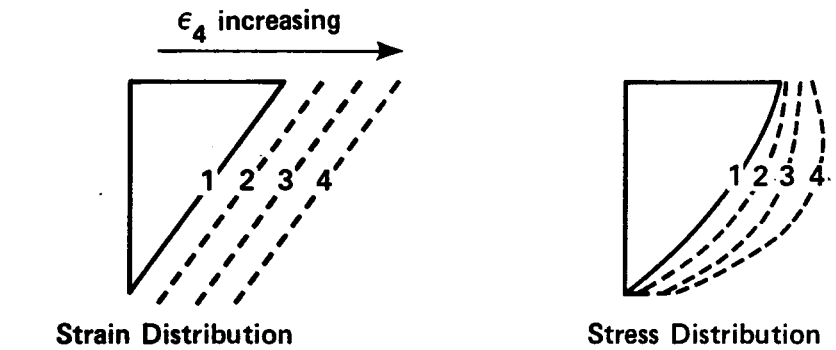

(a) ϵ_4 increasing

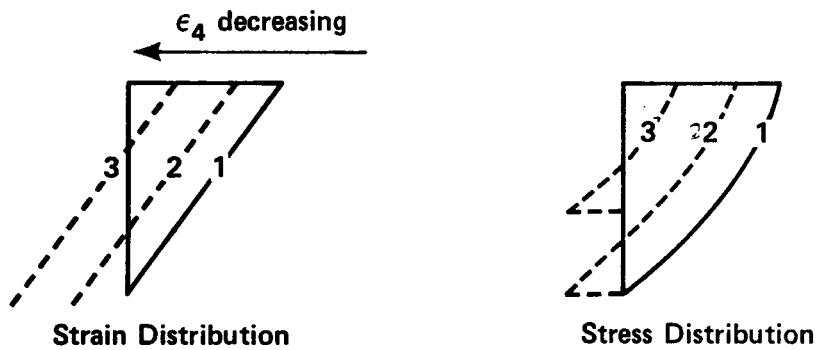

(b) ϵ_4 decreasing

Figure 3.10 Changes in Stress Distribution as ϵ_4 Increases and Decreases

could become negative as shown in Figure 3.9. The inflection point appeared to correspond to the condition of zero strain at the bottom of the section.

The strain distribution with zero strain on the tensile side was chosen as the starting reference point for the first curvature. The forces due to these strains as well as the resultant force, P_{ref}, were then calculated, as described in Section 3.5. Once the coordinates of the reference point are known, ε_4 is given a small increment, $\Delta\varepsilon_4$, as shown in Figure 3.11, and the coordinates of this point are calculated. The slope between these two points is then calculated using:

$$\frac{\delta P}{\delta \varepsilon_4} = \frac{P_a - P_{ref}}{\Delta \varepsilon_4} \tag{3.11}$$

The correction to ε_4, ε_{cor}, is determined by going along this slope to the desired level of P as described by the following equation and as shown graphically in Figure 3.11.

$$\varepsilon_{cor} = \frac{P_{desired} - P_{ref}}{\delta P/\delta \varepsilon_4} \tag{3.12}$$

For prestressed concrete beams, the desired P is zero since there is no external axial force on the beams. The value of P is calculated for this new corrected value of ε_4. This P is then compared to the tolerance level. If it is close enough to zero, no further iterations are required. If not, this corrected point is taken as the reference point

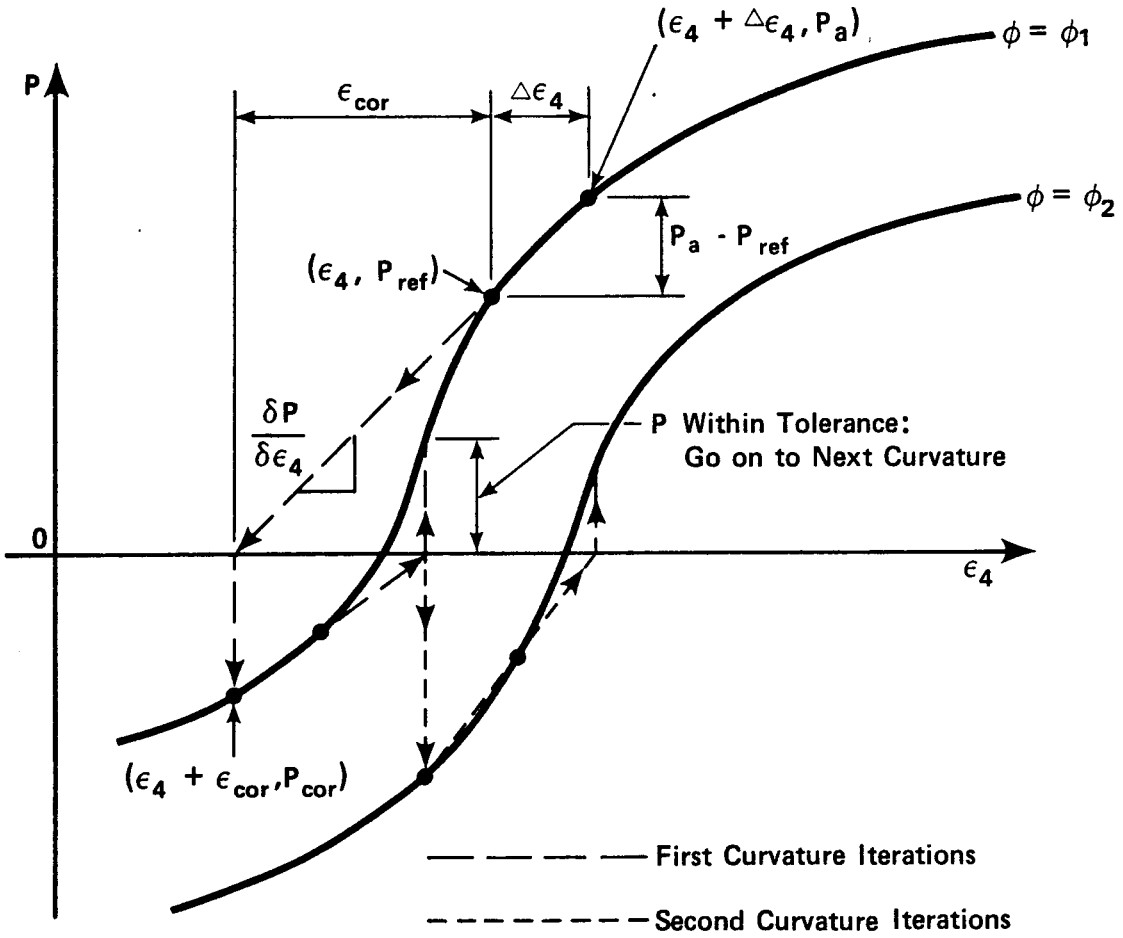

Figure 3.11 Illustration of Newton-Raphson Technique

and the process of incrementing ε_4, getting a slope, and then shooting along this slope is repeated.

Once the value of P is within the allowable tolerance, the moment due to this strain distribution can be found and thus one point on the M–ϕ curve has been determined. The curvature is then incremented and the "correct" ε_4 from the previous curvature is used as the starting point on this new P–ε_4 curve as shown in Figure 3.11.

Some problems were encountered with the Newton-Raphson procedure in connection with the incrementing of curvature. If the increment was too large, the Newton-Raphson procedure would tend to "shoot" to a corrected ε_4 that was close to, or greater than, the ultimate strain, ε_u. Due to the shape of the P–ε_4 curve in this region, the calculated slope for the next correction was either flat, as shown in Figure 3.12(a), or so slight that a negative value of ε_4 resulted, as in Figure 3.12(b). A reduction in the size of the increment in curvature corrected these problems, as shown by the dotted curves in these figures.

The Newton-Raphson technique was found to break down in a few other cases. These problems did not have anything to do with the increment of curvature. One case, shown in Figure 3.13(a), occurs when the corrected value of ε_4 corresponded to a P that was farther away from zero than the starting P. The value of ε_4 may not converge to the solution when this occurs. Another case occurs when the Newton-Raphson method oscillated back and forth between two points

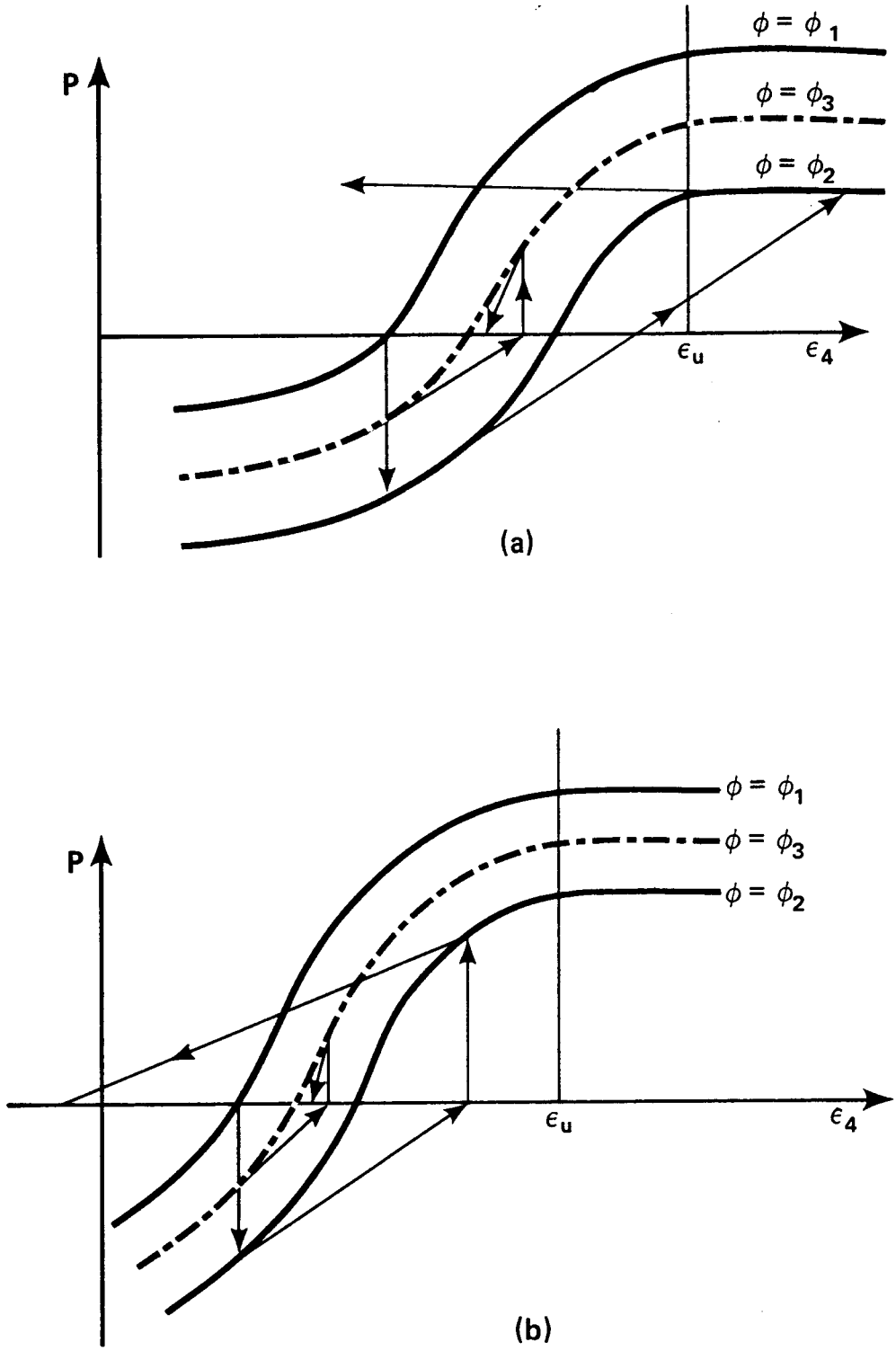

Figure 3.12 Problems with Incrementing Curvature

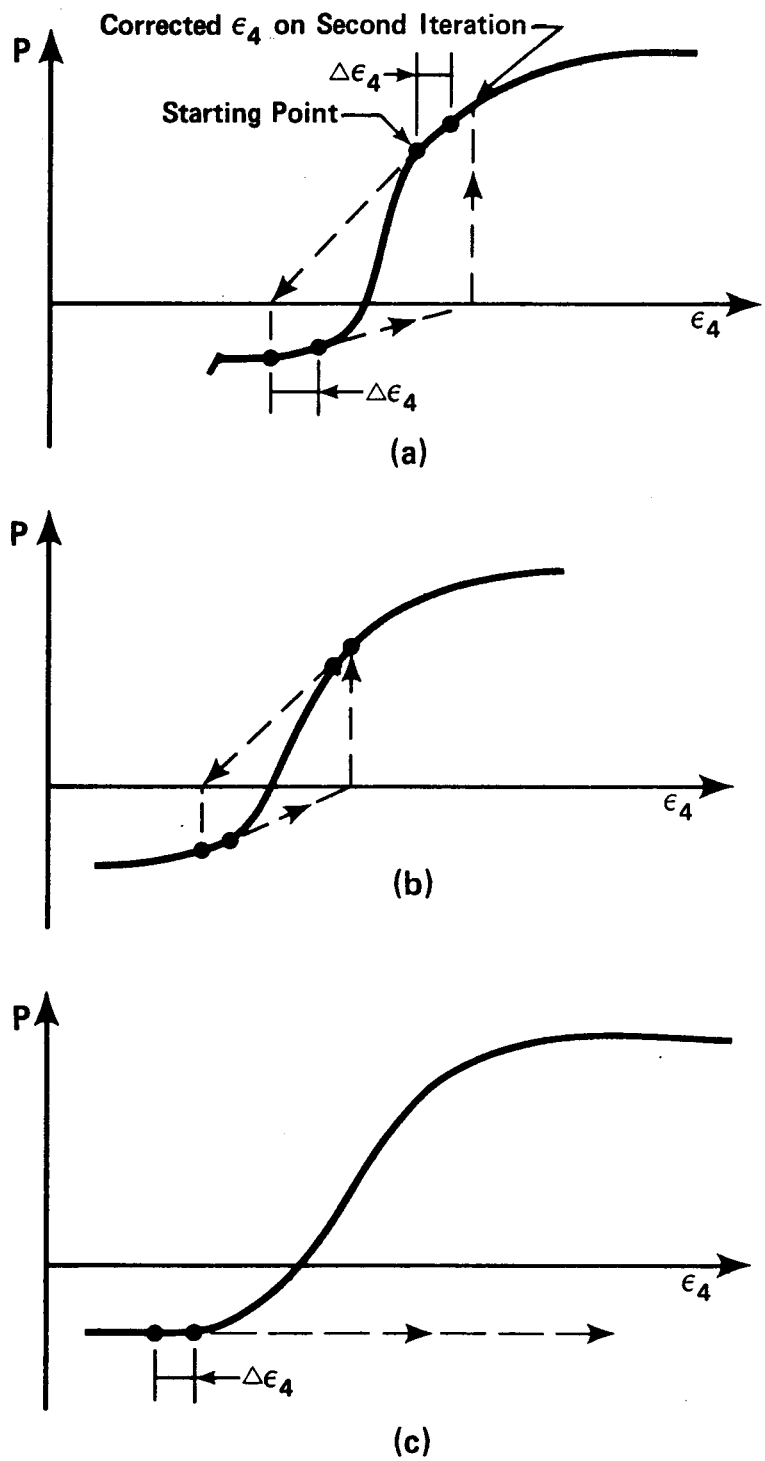

Figure 3.13 Cases Where Newton-Raphson Procedure Breaks Down

as shown in Figure 3.13(b). Yet another case where this technique cannot be used is when the value of P for ε_4 and the value of P for $\varepsilon_4 + \Delta\varepsilon_4$ are equal. The slope is thus calculated to be zero and the value of ε_{cor} cannot be calculated, as shown in Figure 3.13(c).

When the Newton-Raphson technique breaks down, a trial and error approach is used. This procedure basically increments ε_4 until the forces balance within a specified tolerance. The increment is divided in two every time the sign of P changes and P is still outside the tolerance. Thus the increments become smaller as the method converges on the correct ε_4. This method is shown graphically in Figure 3.14. The value of P is calculated for point 1 first. Since P is outside the tolerance and is negative, the strain ε_4 is increased by adding an increment, $\Delta\varepsilon_4$. Because P for point 2 is still outside the tolerance, $\Delta\varepsilon_4$ is added to the strain at point 2. Going from point 2 to point 3, the sign of P changes and the P at point 3 is still outside the tolerance so the increment is halved and subtracted from point 3. In the figure, point 4 is within the tolerance so the process is stopped. If the tolerance is small or the increments are large, the increment may be halved a number of times.

3.7 ACI Calculation of Ultimate Moment

The calculation of the ultimate moment capacity of prestressed concrete beams according to the ACI Building

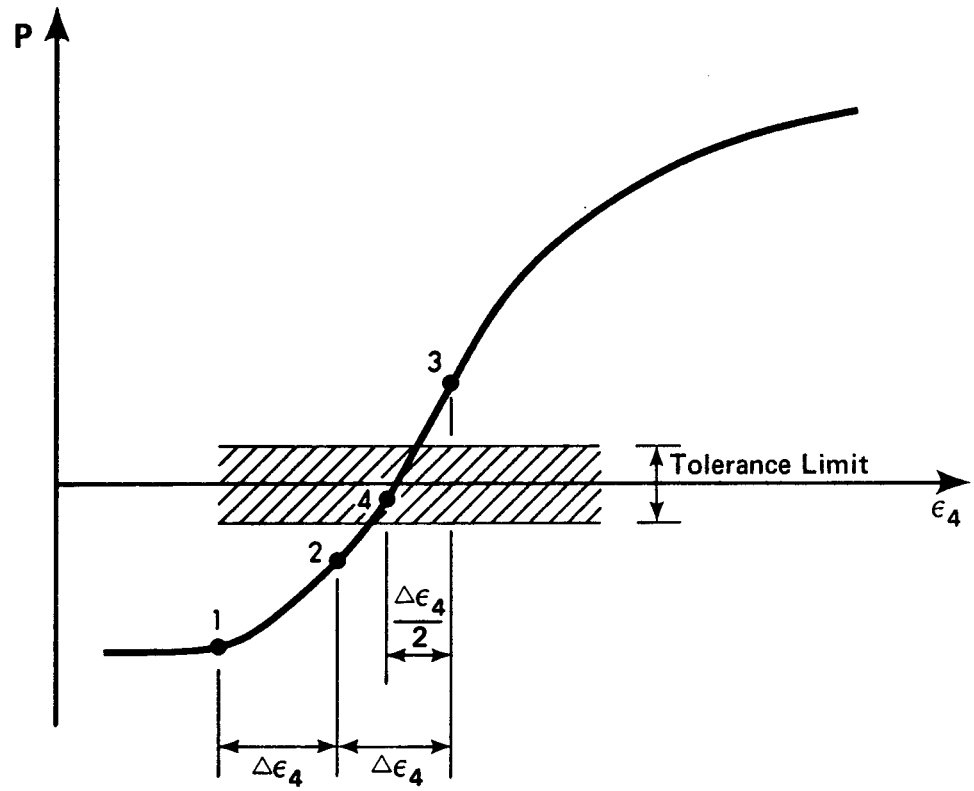

Figure 3.14 Trial and Error Procedure

Code (1971a) is required in this study. This calculation is basically the same as that for reinforced concrete beams. The only difference is that there is a force due to the prestressing steel, as shown in Figure 3.15.

The ACI calculation of ultimate strength is performed by the ACI subroutine in the computer program developed for this study. The rectangular concrete stress distribution as shown in Figure 3.15 is permitted in the ACI Code and was used in these calculations. The depth of the rectangular block was determined from $a = \beta_1 c$ where c is the depth to the neutral axis and β_1 is a constant defined in the ACI Code with a value of 0.85 for strengths, f'_c, up to 4000 psi and which is reduced continuously at a rate of 0.05 for each 1000 psi of strength in excess of 4000 psi. The maximum strain in the extreme concrete compression fiber was assumed to be 0.003 as specified in the ACI Code. The tensile strength of the concrete was neglected. It should be noted that the ACI calculation of ultimate moment in this study did not include any understrength (ϕ) factors.

The effect of conventional reinforcing steel on the ultimate moment was accounted for in the ACI subroutine. Tension reinforcing steel was always assumed to be yielded as allowed in Section 18.7.2 of the ACI Code. Following a check by hand calculations, this assumption was found to be true for all the beams investigated in this study. Any compression reinforcing steel was also assumed to be

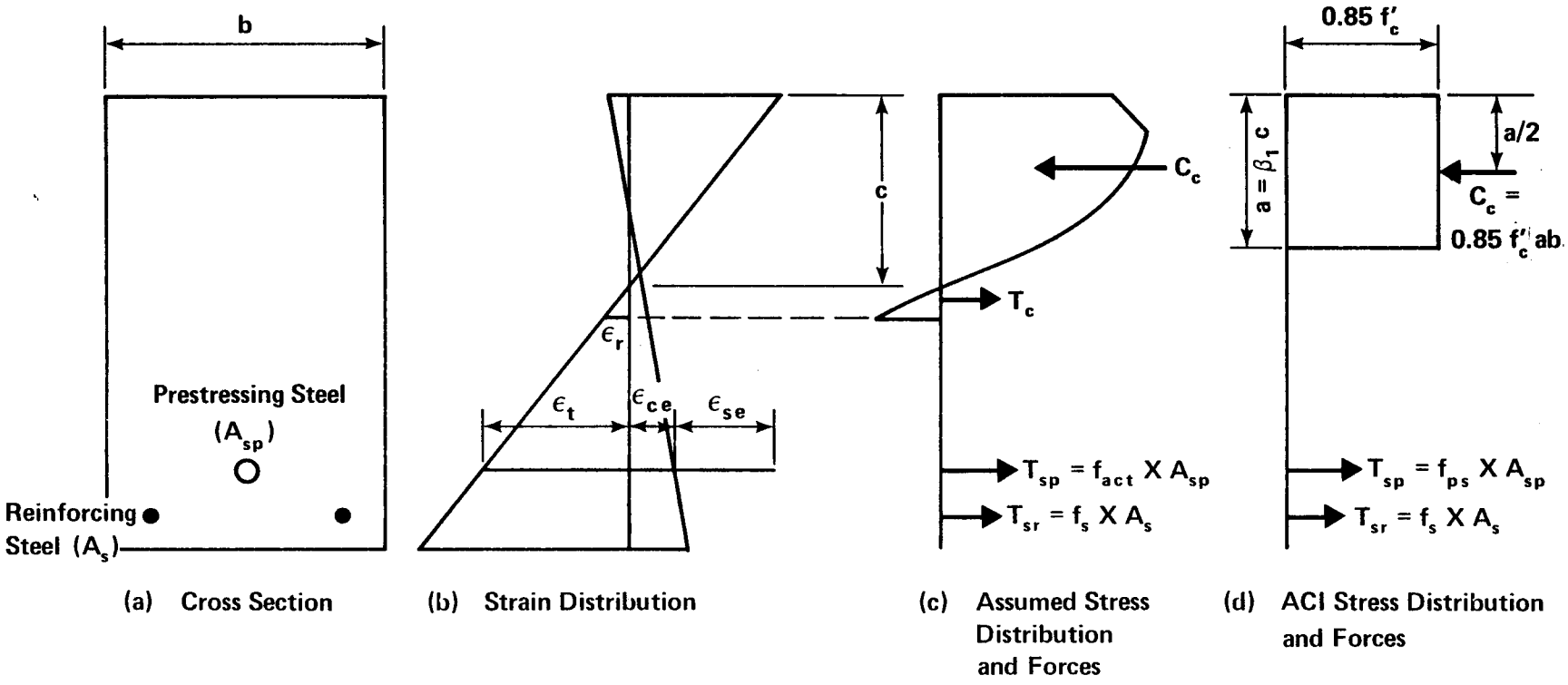

Figure 3.15 Comparison of Assumed and ACI Stress Distributions

yielded but, unlike the assumption for tension steel, this assumption is checked in the ACI subroutine using a strain compatibility analysis. If it was found that the compression steel had not yielded, the stress was set equal to the modulus of elasticity multiplied by the steel strain.

The stress in the prestressing steel at design load, f_{ps}, was determined by using Equation 18-3 of the ACI Code:

$$f_{ps} = f_{pu}\left(1 - 0.5\rho_p \frac{f_{pu}}{f'_c}\right) \qquad (3.13)$$

where:

f_{pu} = ultimate strength of the prestressing steel, psi

$\rho_p = A_{sp}/bd$
= ratio of prestressed reinforcement

f'_c = specified compressive strength of concrete, psi.

This equation is an approximation and can only be used if f_{se} is not less than $0.5f_{pu}$. However, the mean nominal value of f_{se} was always greater than $0.5f_{pu}$ for the beams investigated in this study. The above equation was used in lieu of a more exact strain compatibility analysis because

the designer would probably use that equation.

As written for this study, the ACI subroutine could handle only one layer of compression steel, one layer of prestressing steel, and one layer of tension reinforcing steel. Thus, if in reality there are three layers of prestressing steel, in the program the prestressing steel must be lumped at the centroid of the three layers.

If prestressing steel and normal tension reinforcing steel are both present, the combined centroid is calculated and the effective depth, d, is defined as the distance from the extreme compression fiber to the combined centroid (ACI Code, 1971a).

The ACI subroutine can determine the ultimate moment for either a rectangular beam or a T-beam. A beam is classified as a T-beam when the total maximum compressive force possible from the concrete in the flange and the compression steel is less than the tension force so that the neutral axis is forced down into the web.

When the compression steel lies within the equivalent rectangular stress block, the area of concrete that is displaced by the steel is accounted for in the program by subtracting the force due to this area from the total compressive force calculated assuming that no concrete is displaced by the steel.

A beam is classified as underreinforced and the ultimate moment is calculated in the normal way only if the steel ratio is less than or equal to 0.30:

$$\omega_p \leq 0.30 \tag{3.14}$$

$$(\omega + \omega_p - \omega') \leq 0.30 \tag{3.15}$$

$$(\omega_w + \omega_{pw} - \omega_w') \leq 0.30 \tag{3.16}$$

where:

$\omega = \rho f_y / f'_c$ (tension reinforcement)

$\omega' = \rho' f_y / f'_c$ (compression reinforcement)

$\omega_p = \rho_p f_{ps} / f'_c$ (prestressing steel) and

$\omega_w, \omega_{pw}, \omega_w'$ = reinforcement indices for flanged sections computed as above except that b is the web width, and the steel area is that required to develop the compressive strength of the web only.

If the steel ratio is greater than 0.30, the beam is classified as overreinforced and the ultimate moment is calculated using the equation (ACI, 1971b):

$$M_u = 0.25 f'_c b d^2 \tag{3.17}$$

This equation underestimates the ultimate moment because there are additional safety factors in this equation due to

the nature of failure of an overreinforced beam. This type of beam fails when the concrete crushes, which is a sudden and dangerous failure.

The ACI Code (1971a) requires that the area of prestressed and nonprestressed reinforcement be sufficient to develop a design load of at least 1.2 times the cracking load. This provision eliminates the possibility of a beam reaching the cracking moment and the ultimate moment simultaneously. This requirement was checked using another ACI program for all the beams studied here. This requirement was not inserted into the ACI subroutine of the Monte Carlo program because it is a design requirement, not an analysis requirement. If this requirement was not met, the section had to be adjusted by adding steel until it was satisfied. Only beams satisfying this requirement were used in the Monte Carlo studies.

CHAPTER IV

PROBABILITY MODELS OF VARIABLES AFFECTING SECTION STRENGTH

The strength of a cross section of a prestressed concrete beam is affected by the variability of the concrete, the reinforcing steel, the prestressing steel, the prestress force and losses, and the dimensions. A probability model is required for each of these variables for use in the Monte Carlo program.

4.1 Concrete Variability

The probability models for the compressive and tensile strengths of concrete and for the modulus of elasticity of concrete were taken from a statistical description of the strength of concrete prepared by Mirza, Hatzinikolas, and MacGregor (1978) and will not be derived here.

The mean 28-day strength of concrete in a structure for minimum acceptable curing was given as:

$$\bar{f}_{cstr_{35}} = 0.675f'_c + 1100 \leq 1.15f'_c \text{ psi} \qquad (4.1)$$

The subscript 35 denotes a rate of loading of 35 psi/sec.

which represents a typical testing rate for a concrete control cylinder.

The effect of different rates of loading should also be taken into account. The higher the rate of loading, the higher the apparent strength. Lower strengths at lower rates of loading are probably due to creep and microcracking effects which have more opportunity to develop when the specimen is loaded slowly. The mean value for the *"in-situ"* or "in-structure" compressive strength at a rate of loading of R psi/sec. was taken as:

$$\bar{f}_{cstrR} = \bar{f}_{cstr_{35}}[0.89(1 + 0.08\log_{10}R)]\text{psi} \qquad (4.2)$$

The coefficient of variation of the *in-situ* strength at a given rate of loading was given by Mirza *et al.* (1978) as:

$$V^2_{cstrR} = V^2_{ccyl} - 0.04^2 + 0.10^2 = V^2_{ccyl} + 0.0084 \qquad (4.3)$$

where V_{ccyl} is the coefficient of variation of the compression test cylinders for a particular job. In the analyses reported in this thesis, pretensioned beams were assumed to be precast, and hence were assumed to have better-than-average to excellent control with V_{ccyl} equal to 10 percent. Post-tensioned beams, on the other hand, were assumed to be cast-in-place with average concrete control, for which V_{ccyl} was taken equal to 15 percent.

The tensile strength of concrete was represented by the model for flexural tensile strength proposed by Mirza *et al.* (1978) in lieu of that for splitting tensile strength. This was done because it was felt that the former better predicted the tensile strength of concrete in a beam. The following two equations were used to describe the tensile strength of concrete:

$$\bar{f}_{rstrR} = 8.3\bar{f}_{cstr35}^{\frac{1}{2}}[0.96(1 + 0.11\log_{10}R)]\text{psi} \qquad (4.4)$$

$$V_{rstrR} = 0.20 \qquad (4.5)$$

The model for the initial tangent modulus of elasticity used the following equations:

$$\bar{E}_{cistrR} = 60{,}400\bar{f}_{cstr35}^{\frac{1}{2}}(1.16 - 0.08\log_{10}t) \qquad (4.6)$$

where t is the loading duration in seconds

$$V_{cistrR} = 0.08 \qquad (4.7)$$

It can be seen from the above equations that the tensile strength and modulus of elasticity depend on the compressive strength. However, these equations by themselves do not prevent the Monte Carlo technique from generating a high value of compressive strength and low values of tensile strength and modulus of elasticity. This would be

unrealistic because, as can be seen from the above equations, a high compressive strength tends to be accompanied by a high tensile strength and a high modulus of elasticity. To prevent unrealistic combinations from occurring, the mean values of tensile strength and modulus of elasticity are set equal to values that depend on the generated value of compressive strength before the random number generating subroutine is used to generate values for tensile strength and modulus of elasticity as described by the following equations:

$$\bar{f}_{rstr35} = 8.3\sqrt{X_1} \tag{4.8}$$

$$\bar{E}_{cistr35} = 60{,}400\sqrt{X_1} \tag{4.9}$$

where X_1 is the generated value of compressive strength at a rate of loading equal to 35 psi/sec. for the particular beam under consideration.

Equations 4.2, 4.4, and 4.6 are then used to apply the rate of loading effects to the generated values. This procedure ensures that if a high value is generated for compressive strength, relatively high values would also be generated for the tensile strength and modulus of elasticity.

The cracking strain, ε_r, is equal to the tensile strength divided by the modulus of elasticity.

The distributions of compressive strength, ten-

sile strength, and modulus of elasticity of concrete were assumed to be normal.

4.2 Reinforcing Steel Variability

An elastic-plastic stress-strain curve was used for the reinforcing steel. Probability models of properties related to reinforcing steel were obtained from a paper on the variability of the properties of reinforcing bars by Mirza and MacGregor (1978a). It should be noted that only Grade 60 bars were considered in the present study.

The mean value and coefficient of variation of the mill test yield strength were 71,000 psi and 9.3 percent, respectively. The probability density function (PDF) of of the mill test yield strength was calculated using a Beta distribution described by:

$$PDF = 7.141\left\{\frac{f_y - 57}{51}\right\}^{2.02} \cdot \left\{\frac{108 - f_y}{51}\right\}^{6.95} \qquad (4.10)$$

where: $57 \leq f_y \text{ (ksi)} \leq 108$

The mill test yield strength is determined at a much greater rate of loading than is normally encountered in the structure. As a result, the yield strength is overestimated. This is corrected by subtracting df_{ys} from the mill test yield strength to get the static yield strength. The distribution of df_{ys} was assumed to be normal with a mean value of 3.5ksi and coefficient of variation of

13.4 percent.

The modulus of elasticity was assumed to be normally distributed with a mean of 29,000 ksi and a coefficient of variation of 3.3 percent.

The actual area of reinforcing steel is usually not equal to the nominal area. This is taken into account by multiplying the nominal area by the ratio of measured to nominal area, A_m/A_n. This ratio is normally distributed and truncated at 0.94 and 1.06. It has a mean value of 0.99 and a coefficient of variation of 2.4 percent.

Because reinforcing steel comes only in certain sizes, the furnished area of steel is usually not equal to the area of steel required by calculations. Therefore, the nominal area of steel is also multiplied by the ratio of furnished to calculated areas, A_f/A_c. A modified log-normal distribution with mean value 1.01, coefficient of variation 4 percent, and modification constant 0.91 was used for this ratio. This distribution was suggested by Mirza and MacGregor (1978b) in their paper "Variations in Dimensions of Reinforced Concrete Members."

4.3 Prestressing Steel Variability

Data pertaining to prestressing strand was obtained from the material test records of Con-Force Products Ltd., Edmonton for 1976 and 1977. This data included 99 and 100 samples, respectively, of Grade 270 stress relieved strand and Grade 270 stabilized strand. The strand was

from two sources in two countries and was in two diameters, 7/16 and 1/2 inch. This data was analyzed statistically as described in this section.

A number of correlation analyses were also performed using this data in an attempt to find interdependence between parameters. No correlation was found between the ultimate strain and the ultimate stress nor between the strain at 70 percent of the ultimate stress and the ultimate strain. A good correlation was found between the stress at 1 percent strain, σ_1, and the ultimate stress, f_{pu}, using a power regression analysis. However, a simpler, linear relationship was found between σ_1 and f_{pu} by dividing the mean value of stress at 1 percent strain by the mean value of ultimate stress to get the coefficient k in the following equation:

$$\sigma_1 = k\, f_{pu} \tag{4.11}$$

where: $k = \dfrac{\overline{\sigma}_1}{\overline{f}_{pu}}$

The results of the correlation analyses were used to help determine what parameters should be used in describing the stress-strain curve for prestressing steel. A number of different parameters with different equations were tried before the stress-strain curve described in Section 3.4 was selected. The stress-strain curve was described using four parameters: the modulus of elasticity, the ratio of the stress at 1 percent strain to the ultimate

stress, the ultimate stress, and the ultimate strain. The mean value and coefficient of variation of each of these four parameters was needed for use in the Monte Carlo program.

The coefficient k in Equation 4.11 was found to be 0.89 for stress relieved strand and 0.90 for stabilized strand. Equation 4.11 was found to fit the data very well; given the measured ultimate stress, this equation yielded values for the stress at 1 percent strain that averaged 0.997 times the measured values of σ_1 with a coefficient of variation 0.014. The coefficient of variation of σ_1/f_{pu} was taken equal to the coefficient of variation of the stress at 1 percent strain which was equal to 1.72 percent. The value of 0.90 for stabilized strand is a reasonable value, borne out by the fact that section 5.6.2 of CSA Standard G279 (1975) uses 90 percent of the minimum breaking strength of the strand as the minimum value for the stress at 1 percent extension for low relaxation strand.

Values for the other three parameters were obtained by comparing the statistical analysis of the Con-Force data with data from the other sources listed in Tables 4.1, 4.2, and 4.3.

It can be seen in Table 4.1 that the mean value of the reported modulus of elasticity from the Con-Force data was 27.58×10^6 psi which was low compared to the American data.* However, the modulus of elasticity calculated from

---

*Private communication not to be identified by company name.

Table 4.1

Modulus of Elasticity* (E_{sp})

TYPE	GRADE	DIAM. (in.)	NO. OF TESTS	MODULUS OF ELASTICITY		SOURCE OF DATA
				MEAN ($\times 10^6$ psi)	COV+ (%)	
STRAND		3/8	25	28.92	2.06	
		7/16	25	29.38	2.11	
		1/2	25	28.52	1.86	American data
	270		9	28.26		
	250		9	28.12		
	250	1/2	20	28.06		
STRESS REL.	270	1/2 & 7/16	79	28.62	1.67	$0.7f_{pu}/\varepsilon_{0.7}$ Con-Force
STRESS REL.	270	1/2 & 7/16	51	27.58	1.50	Reported Con-Force
STABILIZED	270	1/2	100	28.25	1.01	$0.7f_{pu}/\varepsilon_{0.7}$ Con-Force

*Note: Based on Nominal Area
+Note: COV is Coefficient of Variation

RECOMMENDED
OVERALL
3/8"–1/2"

$\overline{E}_{sp} = 28.4 \times 10^6$ psi for Grade 270
$= 28.0 \times 10^6$ psi for Grade 250

COV = 2.0%

Table 4.2

Ultimate Tensile Strength (f_{pu})

TYPE AND SIZE	NO. OF TESTS	ULTIMATE TENSILE STRENGTH				REFERENCE
		MEAN	NOMINAL	MEAN/NOM.	COV+ (%)	
WIRE						
5 mm mill coil	100	1,552	1,530	1.0147	2.54	
5 mm stabilized	100	1,644	1,530	1.0749	3.10	
7 mm mill coil	100	1,674	1,580	1.0592	2.78	Bannister (MPa)
7 mm stabilized	100	1,691	1,580	1.0700	2.24	
7 mm	622	179.5	170	1.0559	2.67	BBR* (kg/mm^2)
Oval A-40	8265	165.12			1.38	Brenneisen and Baus (Germany and
12.2 mm	2698	144.98			1.45	Belgium)
7 mm	499	177.45	170	1.0438	3.16	(kg/mm^2)
7 mm stress rel.	514	163.1	150	1.0873	2.90	
STRAND						
9.5 mm	100	100,196	93,500	1.0716	3.22	
12.7 mm	200	178,062	165,000	1.0792	2.25	
15.2 mm	200	242,428	227,000	1.0680	2.17	Bannister (MPa)
17.8 mm	100	385,305	370,000	1.0414	1.44	
28.6 mm	25	948,360	822,000	1.1537	2.25	
3 x 2.4 mm	380	223	207.09	1.0768	5.83	Brenneisen and Baus (Belgium) (kg/mm^2)
1/2" & 7/16"	99	281,588	270,000	1.0429	1.57	Con-Force (Stress Relieved) (psi)
1/2"	100	279,473	270,000	1.0351	1.17	Con-Force (Stabilized) (psi)

(Continued ↓)

Table 4.2, continued

BARS						
14 mm	1832	107.26			4.1	Brenneisen and Baus (Russia and
16 mm	195	106.26			3.58	Germany)
10 mm	110	112.92			5.0	(kg/mm^2)
12 mm	231	109.46			4.12	
14 mm	275	108.83			5.12	
32 mm	605	109.0			1.92	

+NOTE: COV is Coefficient of Variation
* BBR refers to data provided by Canadian BBR Ltd.

RECOMMENDED OVERALL

$\bar{\sigma}_u$ = 1.04 x Nominal Strength

COV = 2.5%

Table 4.3

Ultimate Strain (ε_{up})

TYPE AND SIZE	NO. OF TESTS	ULTIMATE STRAIN		REFERENCE
		MEAN (IN/IN)	COV+ (%)	
WIRE				
Oval A-40	8265	0.0666	10.5	Brenneisen and Baus (Germany)
12.2 mm	2698	0.0823	8.0	
STRAND				
1/2" & 7/16"	51	0.0480	6.93	Con-Force (Stress Relieved)
BARS				
14 mm	1832	0.0964	18.0	
16 mm	195	0.0954	18.03	
10 mm	110	0.1152	20.06	Brenneisen and Baus (Russia and Germany)
12 mm	231	0.1001	17.8	
14 mm	275	0.0959	20.13	
32 mm	605	0.0980	8.7	

+NOTE: COV is Coefficient of Variation

RECOMMENDED OVERALL

$\bar{\varepsilon}_u = 0.05$ in/in

COV = 7.0%

the Con-Force data by dividing 70 percent of the ultimate stress, $0.7f_{pu}$, by the corresponding strain, $\varepsilon_{0.7}$ agreed very well with that from the American data as shown in Table 4.1. Based on this, the mean value of the modulus of elasticity of Grade 270 strand was taken as 28.4×10^6 psi, with a coefficient of variation of 2.0 percent.

In order to facilitate comparison of ultimate strengths from different sources, the ratio of the mean ultimate strength to the nominal ultimate strength was computed and compared. Table 4.2 shows that this ratio varied from 1.035 to 1.154 for the strand. The Con-Force data fell at the low end of this range and also had slightly lower coefficients of variation than the other sources. The mean value of the ultimate strength was chosen to be 1.04 × nominal ultimate strength for both types of strand, representative of the Con-Force data. The coefficient of variation was chosen to be 2.5 percent. This value is roughly the average of the standard deviations of all of the tests of strand quoted in Table 4.2.

Not much data was available for ultimate strain (Table 4.3). The Con-Force data indicated a mean ultimate strain of 0.05 in/in and a coefficient of variation of 7.0 percent. These values were used for both types of strand.

Based on the data collected and the observation by Brenneisen and Baus (1968) that the mechanical characteristics of prestressing wires, bars, and cables were nor-

mally distributed, all prestressing steel properties were assumed to be normally distributed in this study. An upper and lower limit was set only for the ratio of stress at 1 percent strain to ultimate stress. This would result in a truncated normal distribution. The limits were set at three standard deviations away from the mean value resulting in an upper and lower limit of 0.94 and 0.84 for stress relieved strand, and an upper and lower limit of 0.95 and 0.85 for stabilized strand.

It should be noted that the coefficients of variation for the prestressing steel properties are less than those for the reinforcing steel properties. This is because the production of prestressing steel is a more continuous process than the batch process which is used for reinforcing steel (Bannister, 1968).

It is claimed that stabilized strand has improved stress-strain characteristics compared to stress relieved strand such as a higher modulus of elasticity (Stelco, 1976), a higher proportional limit (Stelco, 1976; Bannister, 1968), as well as a higher ultimate strength and ultimate strain (Bannister, 1968). Due to a lack of quantitative information, however, the same modulus of elasticity, ultimate stress, and ultimate strain were used for both stress relieved and stabilized strand. The data from Con-Force indicated that there was little difference between these values for the two types of strand. As described in Section 3.4, the proportional limit was increased from 70 per-

cent of the ultimate stress for stress relieved strand to 75 percent of the ultimate stress for stabilized strand. Bannister (1968) states that 75 percent is a minimum value for stabilized wire. As mentioned earlier, the ratio of the stress at 1 percent strain to the ultimate stress was increased to 0.90 for stabilized strand from 0.89 for stress relieved strand.

Since the Con-Force test data was based on the nominal areas of the strands, no correction was made to account for the variability of the areas of the strands.

4.4 Variability of Prestressing Losses

4.4.1 Preliminary Investigation

A preliminary investigation was carried out to determine if prestressing losses had a significant effect on the stress in the prestressing steel at ultimate, and hence on the ultimate moment. The stress-strain diagram used in this investigation was obtained from the mean values of the statistical analysis of the prestressing steel data (see Section 4.3). This mean curve was shifted in the negative direction by the initial prestrain, $\varepsilon_{se} + \varepsilon_{ce}$, as shown in Figure 4.1. The meanings of ε_{se} and ε_{ce} are explained in Section 3.1. The magnitude of $\varepsilon_{se} + \varepsilon_{ce}$ was calculated by arbitrarily assuming that losses of 22 percent of the initial transfer stress occurred. The calculation of ε_{se} and ε_{ce} is further described in Section 5.2.

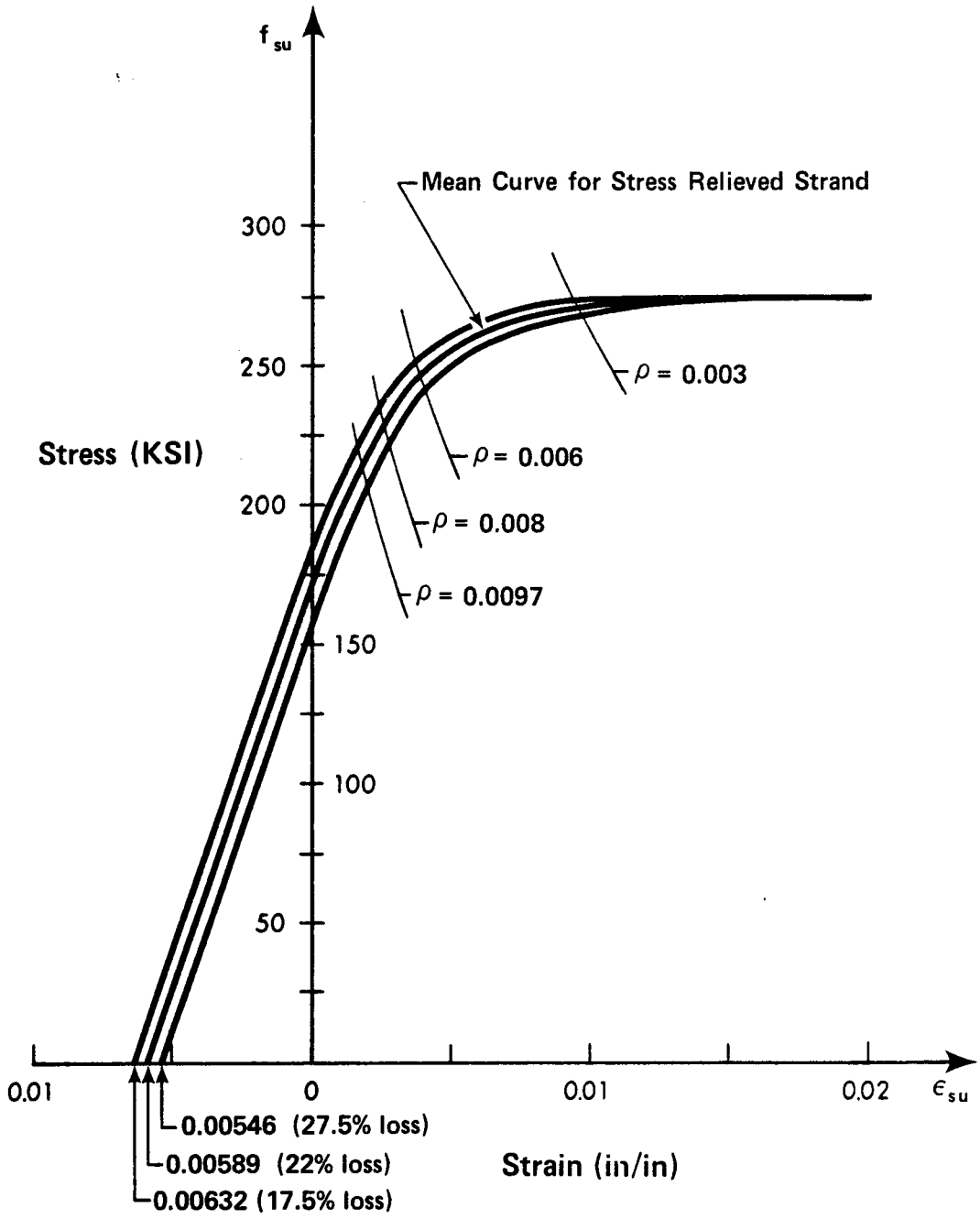

Figure 4.1 Effect of f_{se} on Prestressing Steel Stress At Ultimate

The effect of variations in the losses was arbitrarily studied by multiplying the assumed loss of 22 percent by 1.25 and 0.75 to get 27.5 percent and 16.5 percent losses, respectively. The different amounts of loss resulted in different values of $\varepsilon_{se} + \varepsilon_{ce}$. This in turn shifted the stress-strain curve to either side of the mean curve as shown graphically in Figure 4.1.

Also plotted in this figure is the locus of possible solutions for the stress in the prestressing steel at failure, f_{su}, for varying values of steel ratio, ρ_p. The range of ρ_p was obtained from a survey of the sections listed in the *PCI Design Handbook* (1971). The equation for these curves is:

$$f_{su} = \left(\frac{\beta_1 0.85 f'_c}{\rho_p}\right)\left(\frac{\varepsilon_{cu}}{\varepsilon_{cu} + \varepsilon_{su}}\right) \qquad (4.12)$$

where: β_1 = factor relating the depth of the equivalent rectangular stress block to the neutral axis depth (see Section 3.7).

ε_{cu} = limiting strain in concrete
= 0.003 in *ACI Building Code* (1971a)

ε_{su} = strain in the prestressing steel at failure.

This equation can be derived from strain compatibility and equilibrium (Warwaruk *et al.*, 1962), based on a rectangular stress block. The intersections give stresses at failure.

The difference between the high and low values of

steel stress due to the assumed variation in losses ranged from 1 percent for beams with a prestressing steel ratio $\rho_p = 0.003$ to as much as 6 percent for a steel ratio $\rho_p = 0.01$. Because the latter value appeared significant, prestressing losses were included as a random variable and a probability model for the losses was estimated.

4.4.2 Method of Calculation of Losses

The prestressing losses were calculated for a typical Prestressed Concrete Institute (PCI) beam (8DT 20 with a strand pattern 68-D1) (PCI, 1971) with a span of 50 feet. The strands were assumed to be jacked from one end. The mean loss, maximum loss, and minimum loss calculations were carried out for the four combinations of type of prestressing operation (pretensioned and post-tensioned) and type of prestressing steel (stress relieved and stabilized).

Anchorage loss, elastic shortening loss, and time dependent losses due to shrinkage, creep, and relaxation were all taken into account in these calculations.

Anchorage loss is the loss of stress in the prestressing steel due to the anchorage of the prestressing steel. In post-tensioned members, the anchors at the end of the tendons will slip slightly and locally deform the end of the beam as they set, thus reducing the stress slightly. Anchorage loss in pretensioned members is caused by slippage in the strand-holding devices.

Elastic shortening loss occurs when the pre-

stressing force is applied to the concrete. Under this compressive force, the concrete shortens a bit and the prestressing steel shortens the same amount. Thus, there is a reduction of stress in the steel. This loss occurs in both post-tensioned and pretensioned construction.

As the concrete loses water, it shrinks, resulting in loss of stress in the steel. This loss is called shrinkage loss.

Creep loss occurs as the concrete creeps. Creep is defined as the change in strain which takes place in concrete due to a constant stress. A prestressed beam is not subjected to a constant stress; the stress is always changing as the losses grow in magnitude. Partly for this reason, an incremental approach was used in the calculation of losses. The stress in the concrete at the center of gravity of the steel is the stress that is used in the creep calculations.

Relaxation of the prestressing steel also causes a loss of stress in the steel. Relaxation is defined as the change in stress that takes place due to a constant strain. Generally, relaxation increases as stress, time, and temperature increase. Only normal temperatures (20°C) were considered in this study. Thus, it was assumed that steam curing or any other process that increases the temperature was not used on the typical beam used for the loss calculations.

Due to the different sequence and method of pre-

stressing, the losses for a post-tensioned beam are different from those for a pretensioned beam. In a post-tensioned beam, ducts are placed in position and then the concrete is poured. The concrete is then cured until it is strong enough to withstand the jacking and anchoring of the tendons.

Shrinkage occurs in the concrete during this period of time between pouring and anchoring which was assumed to be fourteen days long in the loss calculations. This shrinkage does not affect the steel stress, however, because the concrete and the strands are still unbonded. When the tendons are jacked, there is a friction loss due to the lack of straightness (wobble) of the ducts. Since only straight tendons were used in this study, the curvature coefficient was omitted from the expression for friction loss:

$$P_s = P_x e^{Kl} \tag{4.13}$$

where: P_s = steel force at jacking end

P_x = steel force at any point x

K = wobble friction coefficient per foot of prestressing steel

l = length of prestressing steel element from jacking end to any point x.

When the tendons are anchored, there is an anchorage loss due to the effect of wedge set. From a literature review,

the mean value of this movement was chosen to be 0.35 inch with a maximum of 0.5 inch and a minimum of 0.2 inch. The stress in the prestressing steel after the tendons are anchored is called the stress at transfer. The elastic shortening loss occurs at transfer. To develop bond between the tendons and the concrete, grout is injected into the ducts at this stage. The time dependent losses—shrinkage, creep, and relaxation—then take place.

In a pretensioned beam, the strands are first stressed in the pretensioning bed. Relaxation losses start from this point. An anchorage loss due to slippage in the strand-holding devices occurs. The Prestressed Concrete Institute (1971) suggests a maximum loss of 5 percent due to slippage and the effect of strand deflection devices. Since straight strands were used in this study, there would be no loss due to deflection devices. A mean anchorage loss of 2.5 percent was chosen, with a maximum of 4.5 percent and a minimum of 0.5 percent. The concrete is then poured around the tendons. After steam curing or a few days of normal curing, the concrete is bonded sufficiently to the strands and has sufficient strength to allow the strands to be released. Shrinkage occurs in the concrete during this period of time which was assumed to be three days long in the loss calculations. Unlike the post-tensioned beam, this preliminary shrinkage does reduce the steel stress because the concrete is bonded to the steel right from the start. An elastic shortening loss occurs at transfer. Time de-

pendent losses then take place.

There is essentially no difference between a post-tensioned beam and a pretensioned beam as far as the calculation of the elastic shortening and time dependent losses is concerned. A post-tensioned beam after anchoring and grouting behaves similarly to a pretensioned beam in which the strands are cut. In fact, Khachaturian and Gurfinkel (1969) suggest that losses measured from transfer may be taken as 25,000 psi for both post-tensioned and pretensioned beams.

The mean loss was calculated first. The mean properties of concrete and prestressing steel, described in Sections 4.1 and 4.3, respectively, were used in these calculations. It was assumed that the stress at transfer, $f_{transfer}$, was 70 percent of the specified ultimate stress, $f_{specified}$. Any losses that occur before transfer were compensated for by overtensioning the tendons to an initial jacking stress that was greater than the stress at transfer. The mean value of initial jacking stress in the prestressing steel was calculated by working backwards from the stress at transfer using a trial and error approach. In this calculation, the initial jacking stress was estimated. From this value, the mean friction loss (for post-tensioned beams), the mean shrinkage and relaxation losses during the period prior to transfer (for pretensioned beams), and the mean anchorage loss were subtracted to get the stress at transfer. This trial and error calculation was repeated

until $f_{transfer}$ was approximately 70 percent of $f_{specified}$.

Starting from $f_{transfer}$ and using common elastic theory, the elastic shortening loss was then calculated (PCI, 1971):

$$L_{es} = \frac{E_{sp}}{E_c}(f_{cs})$$

$$= \frac{E_{sp}}{E_c}\left(\frac{P_o}{A_c} + \frac{P_o e^2}{I_g} - \frac{M_{dl} e}{I_g}\right) \qquad (4.14)$$

where: L_{es} = loss of prestress due to elastic shortening

f_{cs} = concrete stress at the centroid of the strand

P_o = prestress force at transfer

A_c = area of concrete

e = eccentricity at point of consideration

I_g = gross moment of inertia of section

M_{dl} = moment due to dead load of the member

The elastic shortening loss for pretensioned beams can be calculated directly from this equation. For post-tensioned beams, the elastic shortening loss calculated in this manner must be adjusted to take into account the effects of stressing tendons one at a time. As each tendon is stressed, the concrete shortens a bit more, resulting in more elastic shortening loss in the steel. The first tendon that is stressed would have the highest elastic shortening loss since the stressing of each subsequent tendon contributes to its loss of prestress. On the other hand, the last tendon that is stressed would have no loss due to elastic

shortening because the shortening in the concrete and steel would have already occurred by the time the prestress was being measured in the last tendon. An average loss for all the tendons is generally used for post-tensioned beams.

The mean time dependent losses were calculated next. Creep and shrinkage losses were determined using the *Comité Européen du Bêton* prediction equations and curves (Neville, 1970). These curves give coefficients which allow one to calculate the 5th and 95th percentiles as well as the mean values of shrinkage and creep. A water cement ratio of 0.5 was assumed for all calculations. The creep and shrinkage calculations require the use of an equivalent thickness, d_m, defined as the ratio of cross sectional area to semi-perimeter. For T-sections, the equivalent thickness was based on the dimensions of the stems because that is where the prestressing steel is located. A relative humidity of 40 percent was assumed for the calculation of mean losses. As explained earlier, the age at transfer, which was taken to be the age at loading for the creep calculations, was taken as fourteen days for post-tensioned beams and three days for pretensioned beams.

The relaxation loss was determined using the graphs for the range of losses for stress relieved strand and stabilized strand given by Stelco (1976). The maximum and minimum values from these bands, as well as the mean value calculated from these values, were used because the customary relaxation formulae tend to overestimate the mean

relaxation losses for strand (Stelco, 1976).

Before maximum or minimum losses could be calculated, the maximum and minimum jacking forces had to be determined. Using data obtained from stressing records for the Edmonton plant of Con-Force Products Ltd., a statistical analysis of the ratio of the actual jacking pressure to the specified jacking pressure was carried out. A mean of 1.030 and a coefficient of variation of 0.0132 were obtained. The maximum and minimum jacking forces were calculated by adding and subtracting three standard deviations from the mean jacking force calculated earlier by trial and error.

A value that is three standard deviations from the mean corresponds to a chance of occurrence of about 1 in 1000. Because the jacking force is independent of the variability of the concrete and steel properties, the chance of getting the maximum or minimum jacking force is about 1 in 1000. On the other hand, the magnitude of the losses depend on both the concrete and steel properties. The maximum and minimum values for these properties were taken as the mean plus or minus 1.645 standard deviations corresponding to the 5th and 95th percentile values, or a chance of occurrence of 1 in 20. The chance of getting maximum (or minimum) concrete and steel properties at the same time is about $1/20 \times 1/20 = 1/400$. This is the same order of magnitude as the chance of getting the maximum or minimum jacking force. The values of the variables

used for the loss calculations are summarized in Table 4.4.

The maximum loss was calculated by using low values of the modulii of elasticity of concrete and steel. Minimum slip and friction losses were subtracted from the maximum jacking force in order to obtain a high stress at transfer and, as a result, the maximum time dependent losses. Mean values were used for all creep and shrinkage coefficients except that the 95th percentile values were taken for the effects of water cement ratios and relative humidity. A relative humidity of 40 percent was used for maximum loss calculations. The upper limit on relaxation losses was taken from the Stelco (1976) literature.

The higher strength properties of concrete and steel (i.e. mean plus 1.645 standard deviations) were used in the calculations for minimum loss. Starting at the minimum jacking force, higher slip and friction losses were subtracted in order to minimize time dependent losses. Mean values were used for all creep and shrinkage coefficients except that the 5th percentile values were used for the terms reflecting the effects of water cement ratio and relative humidity. A relative humidity of 90 percent was used for minimum loss calculations. The relaxation losses were based on the minimum losses suggested by Stelco (1976).

The strength gain of concrete with time was taken into account for pretensioned beams:

Table 4.4

Values of Variables Used in Loss Calculations

VARIABLE	MEAN LOSSES	MAXIMUM LOSSES	MINIMUM LOSSES
JACKING FORCE	31.47 k	32.71 k	30.23 k
STEEL PROPERTY E_{sp}	28.62×10^6 psi	27.83×10^6 psi	29.40×10^6 psi
CONCRETE PROPERTY E_{cc}			
(f'c = 4000 psi) (post-tensioned)	3.723×10^6 psi	2.995×10^6 psi	4.451×10^6 psi
(f'c = 4500 psi)	3.885×10^6 psi	3.125×10^6 psi	4.645×10^6 psi
(f'c = 5000 psi	4.04×10^6 psi	3.25×10^6 psi	4.83×10^6 psi
FRICTION LOSS k (post-tensioned)	0.00125	0.0005	0.002
ANCHORAGE LOSS SLIP			
(post-tensioned)	0.35"	0.2"	0.5"
(pretensioned)	2.5%	0.5%	4.5%
CREEP LOSS			
α_f	0.75	0.75	0.75
β_f	0.85	0.85	0.85
ϕ_0	3.2	3.8	1.25
ξ	1.2 for post-tensioned, 1.6 for pretensioned		
ρ_{time}	varies with time-used mean value line		
SHRINKAGE LOSS			
ψ	400×10^{-6}	550×10^{-6}	15×10^{-6}
α_r	0.76	0.76	0.76
B_r	1.2	1.4	0.95
RELAXATION LOSS	used Stelco Graphs (1976)		

f'c	days after pour
4000	3
4500	10
5000	17

The corresponding gain in modulus of elasticity can be seen in Table 4.4. Because post-tensioned beams were assumed to be cured for fourteen days before they were stressed, a constant strength and modulus of elasticity for concrete was used.

If steam curing was used, the strength gain of concrete would be accelerated so that the concrete would reach a higher fraction of final strength at an earlier period of time. This would tend to decrease the creep loss. Neville (1970) suggests that a fictitious age based on the maturity of the concrete be used in the calculation of creep loss. Steam curing would also raise the relative humidity of the storage which decreases the creep and shrinkage losses. Moist curing would raise the relative humidity so that creep and shrinkage losses would both decrease but would not accelerate the strength gain.

The losses were calculated using the numerical integration procedure presented by Libby (1971). The losses were calculated for a period of five years because most of the losses have occurred by this time and because the beam may be overloaded at any time in its life so that a forty-year loss would tend to overestimate losses at the hypothetical overloading. The results of the loss calculations are given in Tables 4.5, 4.6, 4.7 and 4.8. An

Table 4.5

Summary of Losses*
Post-Tensioned Beam with Stress Relieved Strand

TYPE OF LOSS	MAX.	MIN.	MEAN	$\frac{\text{MIN + MAX}}{2}$
EL. SHORTENING	1.69	0.87	1.24	1.28
SHRINKAGE	5.12	0.10	3.42	2.61
CREEP	9.40	1.68	5.88	5.54
RELAXATION	10.68	6.30	8.36	8.49
SUBTOTAL	26.90	8.95	18.91	17.92
FRICTION	1.42	5.08	3.34	3.25
ANCHORAGE	3.32	7.39	5.49	5.36
FRICTION + ANCHORAGE	4.74	12.48	8.83	8.61
ALL LOSSES	31.64	21.43	27.74	26.53

*All losses in percentage of nominal stress at transfer which is equal to $0.7f_{specified}$.

Table 4.6

Summary of Losses*
Post-Tensioned Beam with Stabilized Strand

TYPE OF LOSS	MAX.	MIN.	MEAN	$\frac{\text{MIN + MAX}}{2}$
EL. SHORTENING	1.69	0.87	1.24	1.28
SHRINKAGE	5.12	0.10	3.42	2.61
CREEP	10.51	1.83	6.50	6.17
RELAXATION	2.44	1.40	1.90	1.92
SUBTOTAL	19.76	4.20	13.07	11.98
FRICTION	1.42	5.08	3.34	3.25
ANCHORAGE	3.32	7.39	5.49	5.36
FRICTION + ANCHORAGE	4.74	12.48	8.83	8.61
ALL LOSSES	24.5	16.67	21.90	20.59

*All losses in percentage of nominal stress at transfer which is equal to $0.7f_{specified}$.

Table 4.7

Summary of Losses*
Pretensioned Beam with Stress Relieved Strand

TYPE OF LOSS	MAX.	MIN.	MEAN	$\frac{\text{MIN + MAX}}{2}$
EL. SHORTENING	1.80	1.08	1.36	1.44
SHRINKAGE	6.60	0.13	4.22	3.36
CREEP	12.01	2.77	8.09	7.39
RELAXATION	6.52	4.31	5.36	5.42
SUBTOTAL	26.93	8.29	19.04	17.61
RELAXATION + SHRINKAGE	5.59	2.42	4.13	4.00
ANCHORAGE	0.55	4.62	2.67	2.59
RELAX. + SHR. + ANCHORAGE	6.14	7.04	6.80	6.59
ALL LOSSES	33.07	15.33	25.84	24.20

*All losses in percentage of nominal stress at transfer which is equal to $0.7f_{specified}$.

Table 4.8

Summary of Losses*
Pretensioned Beam with Stabilized Strand

TYPE OF LOSS	MAX.	MIN.	MEAN	$\frac{\text{MIN + MAX}}{2}$
EL. SHORTENING	1.82	1.06	1.36	1.44
SHRINKAGE	6.60	0.13	4.22	3.36
CREEP	12.89	2.83	8.51	7.86
RELAXATION	1.34	0.86	1.10	1.10
SUBTOTAL	22.64	4.88	15.19	13.76
RELAXATION + SHRINKAGE	2.36	0.63	1.65	1.50
ANCHORAGE	0.54	4.51	2.61	2.52
RELAX. + SHR. + ANCHORAGE	2.90	5.14	4.26	4.02
ALL LOSSES	25.54	10.02	19.45	17.78

*All losses in percentage of nominal stress at transfer which is equal to $0.7f_{specified}$.

example calculation is given in Appendix B.

Because the loss computations were deterministic calculations, each based on a particular low or high value of each of the variables, the probability of the occurrence of the particular high or low losses computed is considerably less than the 1 in 20 assumed for some of the variables. The combinations chosen are felt to result in realistic upper and lower bounds for prestressing losses. For the purposes of computing the coefficient of variation of the losses, the high and low values were arbitrarily assumed to be plus and minus three standard deviations from the mean.

4.4.3 Summary of Losses and Comparison with Other Sources

A summary of the stress at transfer and mean losses occurring after transfer is given in Tables 4.9 and 4.10. For the Monte Carlo study, the mean stress at transfer was taken as 70 percent of the specified ultimate stress for all combinations of type of prestressing operation (pretensioned and post-tensioned) and type of strand (stress relieved and stabilized). The coefficient of variation of the stress at transfer varied only according to the type of prestressing operation, having values of 1.5 percent and 2.0 percent for pretensioned and post-tensioned beams, respectively. The mean losses and the coefficients of variation of losses were found to be

Table 4.9

Stress at Transfer

	STRESS RELIEVED	STABILIZED	RECOMMENDED (FOR STRESS RELIEVED AND STABILIZED)
MEAN STRESS AT TRANSFER	0.7 x specified ultimate	0.7 x specified ultimate	0.7 x specified ultimate
COV*—PRETENSION	0.0143	0.0142	0.015
—POST-TENSION	0.0193	0.0193	0.020

*Coefficient of Variation

Table 4.10

Losses

	PRETENSIONED	POST-TENSIONED	RECOMMENDED (FOR PRETENSIONED AND POST-TENSIONED)
STRESS RELIEVED			
MEAN LOSSES	0.190 x mean stress at transfer	0.189 x mean stress at transfer	0.19 x mean stress at transfer
COV*	0.163	0.159	0.16
STABILIZED			
MEAN LOSSES	0.152 x mean stress at transfer	0.131 x mean stress at transfer	0.14 x mean stress at transfer
COV*	0.195	0.198	0.20

*Coefficient of Variation

similar for pretensioned and post-tensioned beams when expressed as losses measured from transfer. This result supports Khachaturian's statement (1969) that there is no difference between losses measured from transfer for a pretensioned beam and a post-tensioned beam. There was a distinct difference between the losses for stress relieved strand and stabilized strand, however. Thus, the mean loss for stress relieved strand was taken as 19 percent of the mean stress at transfer with a coefficient of variation of 16 percent. The mean loss for stabilized strand was taken as 14 percent of the mean stress at transfer with a coefficient of variation of 20 percent. It should be noted that all losses in these tables are in terms of percent of mean stress at transfer—not initial jacking stress.

Based on a somewhat different method of analysis, Glodowski and Lorenzetti (1972) predicted total prestress losses in 40 years of 21.9 percent and 18 percent, respectively, for stress relieved and stabilized strand. If it is assumed that 90 percent of this would occur in the first five years, the corresponding five-year losses would be 19.7 and 16.2 percent which are close to the values of 19 and 14 percent in the last column of Table 4.10.

The ACI-ASCE Joint Committee 323 (1958) recommended using losses of 35,000 psi for pretensioned beams and 25,000 psi for post-tensioned beams. These losses do not include losses due to friction but they are measured from the time of tensioning—not from when the stress is trans-

ferred to the beam. Thus, the 35,000 psi for pretensioned beams includes relaxation and shrinkage losses that occur between the time of stressing and the time that the stress is transferred. This committee also states that the magnitude of the loss does not significantly affect the ultimate moment.

Lin (1955) gives prestressing losses for both pretensioned and post-tensioned beams with stress relieved strand. These losses are tabulated in Table 4.11. Lin's relaxation losses are quite a bit lower than the relaxation losses calculated in this study because Lin has assumed that the strands have been overtensioned to reduce relaxation losses. Lin (1955) states that ". . . creep may easily be cut in half if it is overtensioned by 5 to 10% and held there for 2 to 3 minutes." No overtensioning has been assumed for the calculations in this study. If the absence of overstressing was assumed to double the relaxation losses, Lin's final losses would be 18 percent for post-tensioned beams and 20 percent for pretensioned beams. This compares favorably with the loss calculations in this study which indicate a loss of 19 percent for both pretensioned and post-tensioned beams.

Overtensioning to reduce relaxation losses was not considered in this study because the effectiveness of this procedure is open to some doubt. The effect of overtensioning was investigated by Magura, Sozen and Siess (1962). After performing some tests of their own as well

Table 4.11

COMPARISON OF LOSS CALCULATIONS
WITH LIN'S LOSSES

TYPE OF LOSS	POST-TENSIONED		PRETENSIONED	
	CALCULATIONS	LIN	CALCULATIONS	LIN
EL. SHORTENING	1.24%	1%	1.36	3
SHRINKAGE	3.42	6	4.22	7
CREEP	5.88	5	8.09	6
RELAXATION	8.36	3	5.36	2
TOTAL	18.91	15	19.04	18

β_r = 1.2 (mean for ratio)

$S = 400 \times 10^{-6} \times 0.75 \times 1.2 \times (1 - 10 \times 5.464 \times 10^{-4})$

$S = 3.628 \times 10^{-4}$

$f_{ss} = 3.628 \times 10^{-4} \times 28.617 \times 10^{3} \times \rho_{time}$

$f_{ss} = 10.382 \rho_{time}$ (ksi)

Relaxation Loss (for stress relieved strand)

TIME (HOURS)	MAX	MIN	MEAN
7 x 24 = 168	0.047	0.029	0.038
14 x 24 = 336	0.054	0.034	0.044
30 x 24 = 720	0.062	0.039	0.0505
90 x 24 = 2160	0.074	0.048	0.061
360 x 24 = 8640	0.087	0.058	0.0725
1825 x 24 = 43,800	0.104	0.071	0.0875

$\therefore$ at 7 days:

$f_{sc} = 1.445 \times 10^{-2} \times 1102.6 \times 1.2 \times 0.21 = 4.015$ ksi

$\Delta f_{sc} = 4.015$ ksi

$f_{ss} = 10.382 \times 0.34 = 3.53$ ksi

$\Delta f_{ss} = 3.53 - 3.11 = 0.42$

$\Delta f_{s\dagger} = 186.7 \times 0.038 = 7.09$ ksi

$f_{s\dagger} = 186.7 - 7.09 = 179.6$ ksi

$\Delta f_s = 4.015 + 0.42 + 7.09 = 11.52$ ksi

$\Delta f_{cgs} = -13.22 \times 11.52 = -152.3$ psi

$f_{cgs} = 1102.6 - 152.3 = 950.3$ psi

at 14 days:

$\Delta f_{sc} = 1.445 \times 10^{-2} \times 950.3 \times 1.2 \times (0.3 - 0.21)$

$= 1.483$ ksi

$\Delta f_{ss} = 10.382\ (0.4 - 0.34)$

$= 0.62$ ksi

$\Delta f_{s\dagger} = 179.6(0.044 - 0.038) = 1.08$ ksi

$f_{s\dagger} = 179.6 - 1.08 = 178.5$ ksi

$\Delta f_s = 1.483 + 0.62 + 1.08 = 3.183$ ksi

$\Delta f_{cgs} = -13.22 \times 3.183 = -42.08$ psi

$f_{cgs} = 950.3 - 42.08 = 908.2$ psi

See Table B-1 for summary of calculations.

Calculation of Percentage Loss*:	
Elastic shortening	$\frac{0.360}{28.92} = 1.24\%$
Shrinkage	$\frac{0.99}{28.92} = 3.42\%$
Creep	$\frac{1.70}{28.92} = 5.88\%$
Relaxation	$\frac{2.42}{28.92} = 8.36\%$
Subtotal	$\frac{5.47}{28.92} = 18.91\%$
Friction	$\frac{0.966}{28.92} = 3.34\%$
Anchorage	$\frac{1.588}{28.92} = 5.49\%$
Friction + Anchorage	8.83%
All losses	27.74%

*All losses in percentage of nominal stress at transfer which is equal to $0.7f_{pu}$. (See Table 4.5 for maximum, minimum and mean losses.)

$$\sigma_{fric+anch} = \frac{\max(\text{fric + anch})\text{loss} - \min(\text{fric + anch})\text{loss}}{6}$$

$$= \frac{12.48 - 4.74}{6} = 1.29\% \text{ of nominal transfer stress}$$

$$\sigma_{jacking} = \begin{bmatrix}\text{Coefficient of Variation} \\ \text{of ratio of Actual to} \\ \text{Specified Jacking Force}\end{bmatrix}\begin{bmatrix}\text{ratio of jacking} \\ \text{to transfer force}\end{bmatrix}$$

Table B-1

MEAN LOSSES FOR POST-TENSIONED BEAM WITH STRESS RELIEVED STRAND

Time† Days	ρ_{time} (Shrinkage)	f_{ss} ksi	Δf_{ss} ksi	ρ_{time} (Creep)	ξ	f_{sc} ksi	Δf_{sc} ksi	Δf_{st} ksi	f_{st} ksi	Δf_s ksi	Δf_{cgs} psi	f_{cgs} psi
0	0.3	3.11	--	--	--	0	--	0	186.7	--	0	1102.6
7	0.34	3.53	0.42	0.21	1.2	4.015	4.015	7.09	179.6	11.52	-152.3	950.3
14	0.4	4.15	0.62	0.3	1.2	4.943	1.483	1.08	178.5	3.18	-42.08	908.2
				(0.21)	(1.2)	3.460						
30	0.5	5.19	1.04	0.41	1.2	6.456	1.732	1.16	177.3	3.93	-51.98	856.1
				(0.3)	(1.2)	4.724						-361.2
												494.9
90	0.61	6.33	1.14	0.6	1.2	5.149	1.630	1.86	175.4	4.63	-61.17	433.7
				(0.41)	(1.2)	3.518						
360	0.8	8.30	1.98	0.8	1.2	6.016	1.504	2.02	173.4	5.50	-72.76	360.9
				(0.6)	(1.2)	4.512						
1825	0.92	9.55	1.25	0.92	1.2	5.758	0.751	2.60	170.8	4.60	-60.82	300.1
				(0.8)	(1.2)	5.007						
			6.45				11.12	15.81		33.36		
			×0.153				×0.153	×0.153		×0.153		
			=0.99kips				=1.70kips	=2.42kips		=5.10kips		

†Time is from time of stressing (14 days after concrete cast)

$$= 1.316 \left(\frac{109}{100}\right) = 1.43\% \text{ of nominal transfer stress}$$

$$f_{transfer} = \alpha_{tr} \cdot f_{jacking}$$

Mean stress at transfer = Nominal Value

$$= 0.7 \times \text{specified ultimate} \longleftarrow$$

$$\sigma_{transfer} = \left[\left(\frac{1.29}{100}\right)^2 + \left(\frac{1.43}{100}\right)^2\right]^{\frac{1}{2}}$$

$$= 1.93\% \times \text{Mean stress at transfer} \longleftarrow$$

$$\text{Mean value of losses} = \frac{18.91}{100} \times \text{Mean stress at transfer}$$

$$= 0.19 \times \text{Mean stress at transfer} \longleftarrow$$

$$\sigma_{losses} = \frac{\text{max. loss - min. loss}}{6}$$

$$= \frac{26.90 - 8.95}{6}$$

$$= 3.00\% \text{ of Mean stress at transfer}$$

$$= 0.03 \times \text{Mean stress at transfer} \longleftarrow$$

$$f_{se} = f_{transfer} - \text{losses}$$

APPENDIX C

FLOW DIAGRAMS OF THE MONTE CARLO PROGRAM

This appendix contains flow diagrams of the Monte Carlo Program used in this study including:

The Main Program

Subroutine THEORY

MONTE CARLO PROGRAM

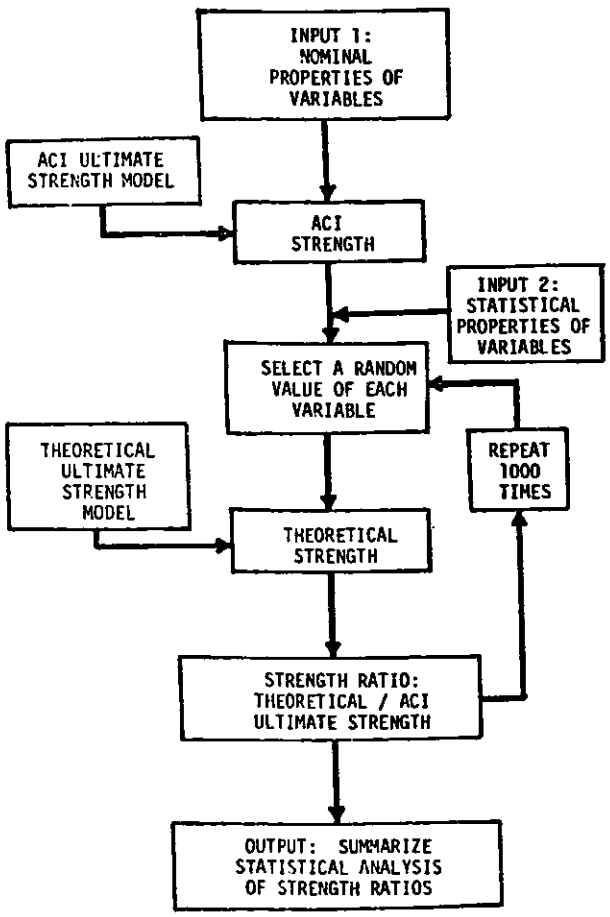

SUBROUTINE THEORY

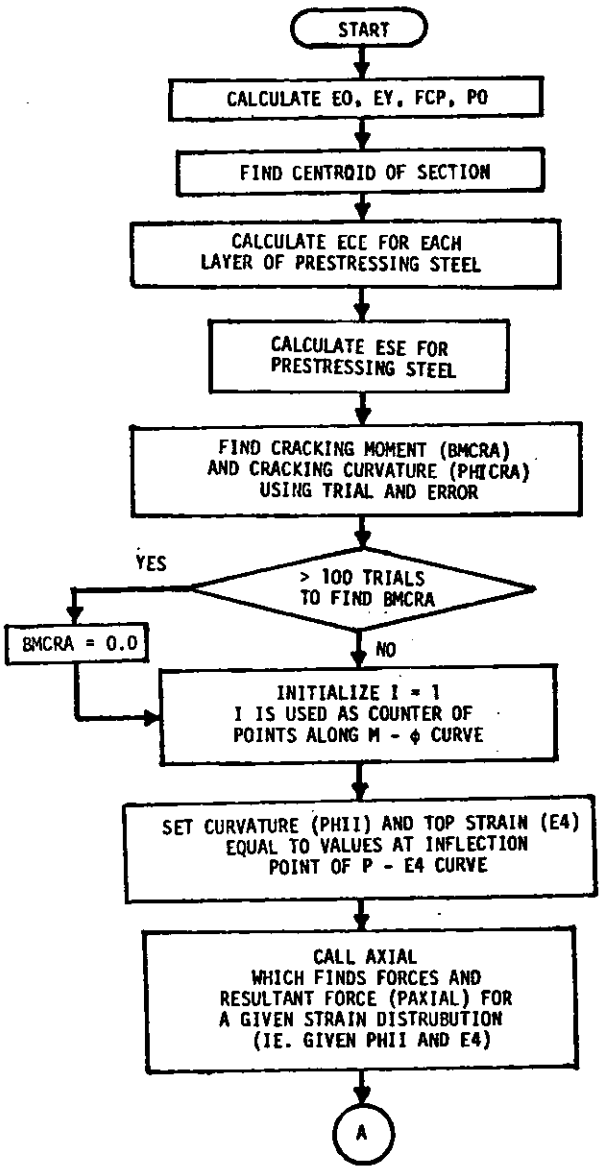

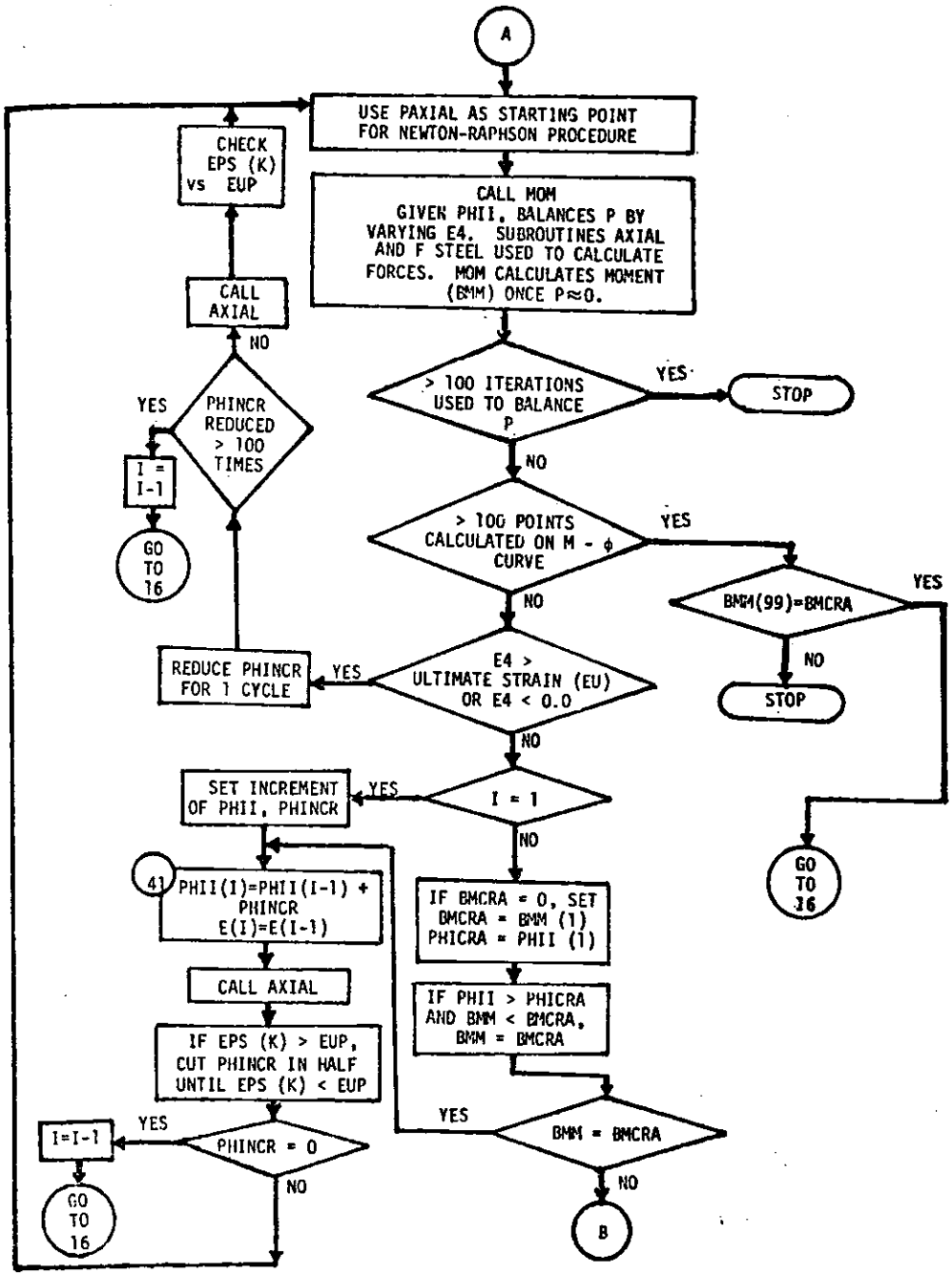
A
USE PAXIAL AS STARTING POINT FOR NEWTON-RAPHSON PROCEDURE
CALL MOM GIVEN PHII, BALANCES P BY VARYING E4. SUBROUTINES AXIAL AND F STEEL USED TO CALCULATE FORCES. MOM CALCULATES MOMENT (BMM) ONCE P≈0.
> 100 ITERATIONS USED TO BALANCE P
YES
STOP
NO
> 100 POINTS CALCULATED ON M - φ CURVE
YES
BMM(99)=BMCRA
YES
NO
STOP
GO TO 16
NO
E4 > ULTIMATE STRAIN (EU) OR E4 < 0.0
YES
REDUCE PHINCR FOR 1 CYCLE
NO
I = 1
YES
SET INCREMENT OF PHII, PHINCR
NO
41
PHII(I)=PHII(I-1) + PHINCR
E(I)=E(I-1)
CALL AXIAL
IF EPS (K) > EUP, CUT PHINCR IN HALF UNTIL EPS (K) < EUP
PHINCR = 0
YES
I=I-1
GO TO 16
NO
IF BMCRA = 0, SET BMCRA = BMM (1) PHICRA = PHII (1)
IF PHII > PHICRA AND BMM < BMCRA, BMM = BMCRA
BMM = BMCRA
YES
NO
B
CHECK EPS (K) vs EUP
CALL AXIAL
NO
PHINCR REDUCED > 100 TIMES
YES
I = I-1
GO TO 16

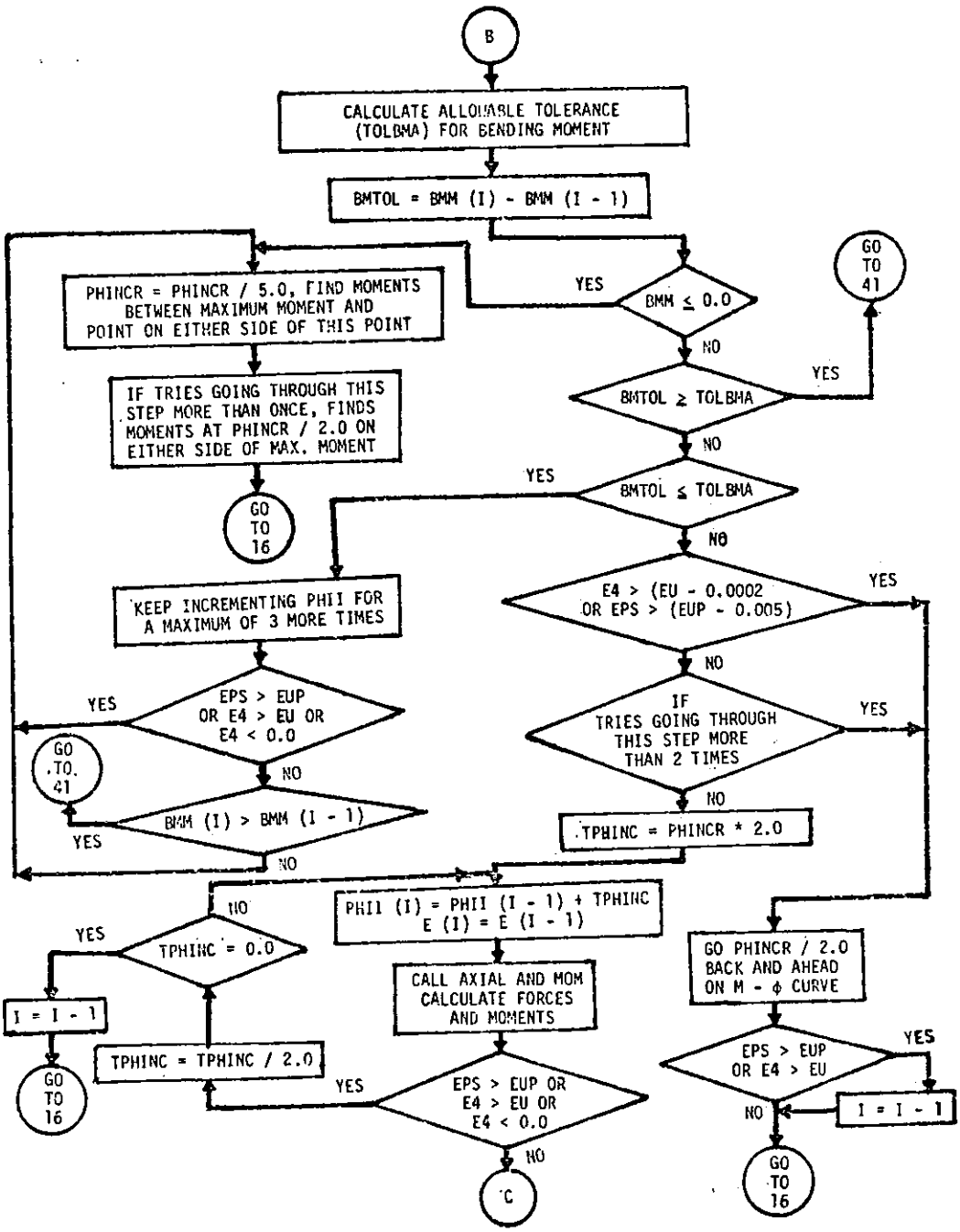
B
CALCULATE ALLOWABLE TOLERANCE (TOLBMA) FOR BENDING MOMENT
BMTOL = BMM (I) - BMM (I - 1)
PHINCR = PHINCR / 5.0, FIND MOMENTS BETWEEN MAXIMUM MOMENT AND POINT ON EITHER SIDE OF THIS POINT
IF TRIES GOING THROUGH THIS STEP MORE THAN ONCE, FINDS MOMENTS AT PHINCR / 2.0 ON EITHER SIDE OF MAX. MOMENT
GO TO 16
BMM ≤ 0.0
YES
NO
GO TO 41
BMTOL ≥ TOLBMA
YES
NO
BMTOL ≤ TOLBMA
YES
NO
KEEP INCREMENTING PHII FOR A MAXIMUM OF 3 MORE TIMES
E4 > (EU - 0.0002 OR EPS > (EUP - 0.005)
YES
NO
EPS > EUP OR E4 > EU OR E4 < 0.0
YES
NO
GO TO 41
BMM (I) > BMM (I - 1)
YES
NO
IF TRIES GOING THROUGH THIS STEP MORE THAN 2 TIMES
YES
NO
TPHINC = PHINCR * 2.0
PHII (I) = PHII (I - 1) + TPHINC
E (I) = E (I - 1)
CALL AXIAL AND MOM CALCULATE FORCES AND MOMENTS
EPS > EUP OR E4 > EU OR E4 < 0.0
YES
NO
C
TPHINC = TPHINC / 2.0
TPHINC = 0.0
NO
YES
I = I - 1
GO TO 16
GO PHINCR / 2.0 BACK AND AHEAD ON M - ϕ CURVE
EPS > EUP OR E4 > EU
YES
NO
I = I - 1
GO TO 16

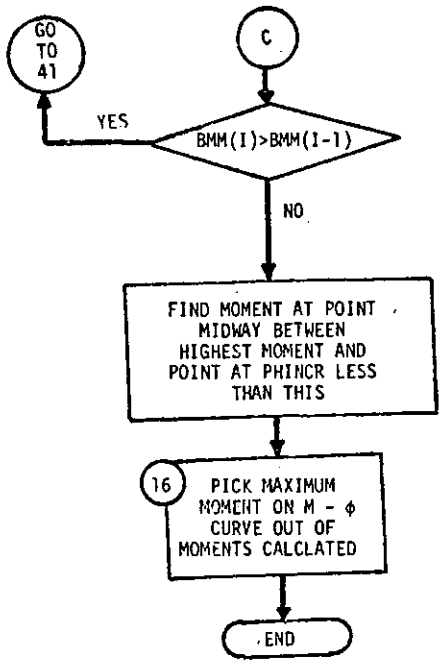
GO TO 41
C
YES
BMM(I)>BMM(I-1)
NO
FIND MOMENT AT POINT MIDWAY BETWEEN HIGHEST MOMENT AND POINT AT PHINCR LESS THAN THIS
16
PICK MAXIMUM MOMENT ON M - φ CURVE OUT OF MOMENTS CALCLATED
END

APPENDIX D

NOMENCLATURE

Alphabetic Symbols

a	depth of equivalent rectangular stress block
A_s	area of conventional reinforcement steel, sq. in.
A_{sp}	area of prestressing steel, sq. in.
b	cross section width on compression face, in.
b_w	width of web, in.
c	depth to neutral axis
C_c	compressive force in concrete, lb.
C_{cs}	compressive force that would have been exerted by concrete that is displaced by compression steel, lb.
C_s	compressive force due to compression reinforcing steel, lb.
d	effective depth, in.
d	depth to tension reinforcing steel, in.

d'	depth to compression reinforcing steel, in.
d_p	depth to prestressing steel, in.
d_t	depth of tension stress block in concrete.
e	eccentricity
E	modulus of elasticity of concrete (used with subscripts given later), psi, (mean value = $\bar{E}$)
E_c	modulus of elasticity of concrete, psi
E_s	modulus of elasticity of reinforcing steel, psi
E_{sp}	modulus of elasticity of prestressing steel, psi
f	strength of concrete (used with subscripts given later), psi, (mean value = $\bar{f}$)
f_{bot}	stress at the bottom of the section
f'_c	specified compressive strength of concrete, psi
f''_c	maximum stress in Hognestad (1952) stress-strain curve for concrete, psi
f_{cu}	the effective stress of the concrete in the compression zone, psi

$f_{jacking}$	stress in the prestressing steel due to the jacking force, psi
f_{ps}	calculated stress in the prestressing steel at design load, psi
f_{pu}	ultimate stress in prestressing steel, psi
f_r	modulus of rupture of concrete, psi
f_{se}	effective stress in prestressing steel, after losses, psi
$f_{specified}$	specified ultimate stress of prestressing steel, psi
f_{su}	prestressing steel stress at ultimate moment, psi
f_{top}	stress at the top of the section
$f_{transfer}$	stress in prestressing steel at transfer
f_y	yield strength of reinforcing steel, psi
F	strain compatibility factor
h	overall depth of cross section, in.
h_f	depth of flange, in.
I	moment of inertia
M	Moment

M_{cr}	cracking moment
M_{dl}	moment due to dead load, psi
M_u	ultimate moment, psi
n	number of prestressing tendons
P	resultant force acting on a cross section, lb.
P_o	prestress force at transfer
P_x	steel force at any point x
T_c	tension force in concrete, lb.
T_{sp}	tensile force due to prestressing steel, lb.
T_{sr}	tensile force due to tension reinforcing steel, lb.
V	coefficient of variation (used with subscripts given later)
$V_{in-batch}$	in-batch variability
V_s	coefficient of variation of the ratio of test strength to theoretical strength
V_{test}	variability due to different people testing and the errors implicit in the test itself
V_{theo}	variability of the theoretical model

y	distance from mid-height to the resultant compressive force in concrete
y_f	distance from mid-height to the resultant compressive concrete force in the flange
y_w	distance from mid-height to the resultant compressive concrete force in the web
Z_b	section modulus with respect to the bottom fiber of a cross section
Z_t	section modulus with respect to the top fiber of a cross section

In addition, the following symbols are used in subscript:

c	refers to "compressive" in conjunction with strength and elastic modulus
ccyl	refers to "compressive cylinders" in conjunction with strength
ci	refers to "initial tangent" in conjunction with modulus of elasticity
g	gross
r	refers to "modulus of rupture with third point loading"
R	refers to "rate of loading R psi/sec" corresponding to strength or modulus of elasticity

$_{str}$ refers to "in-structure or *in-situ*" in conjunction with strength and modulus of elasticity

$_{35}$ refers to "rate of loading 35 psi/sec" corresponding to compressive strength and modulus of elasticity

Greek Symbols

β safety index

β ratio of stress at 1 percent strain to ultimate stress for prestressing steel

β_1 a constant defined in Section 10.2.7 of the ACI Code (1971a)

Δ prediction errors

Δ increment

ε strain, in./in.

ε_{ce} the compressive strain in the concrete due to the prestressing force

ε_{cu} the strain in the extreme concrete fiber in compression at ultimate moment

ε_{ps} the total strain in the prestressing steel, in./in.

ε_r cracking strain in concrete

ε_{se}	effective prestrain in prestressing steel after losses have taken place
ε_{su}	prestressing steel strain at ultimate moment
ε_t	strain at the level of the prestressing tendons
ε_y	yield strain of reinforcing steel
ε_u	ultimate strain in concrete
ε_{up}	ultimate strain in prestressing steel
ε_0	the strain in concrete that corresponds to the maximum stress in Hognestad's (1952) stress-strain curve for concrete
ε_1	the strain at the bottom of the section
ε_3	the strain at the bottom of the flange
ε_4	the strain at the top of the section
λ	overload factor
$\overline{\mu}$	mean value
ρ	ratio of nonprestressed tension reinforcement (= A_s/bd)
ρ'	ratio of nonprestressed compression reinforcement (= A'_s/bd)

ρ_p ratio of prestressed reinforcement (= A_{sp}/bd)

σ standard deviation

σ stress

σ_1 stress at 1 percent strain for prestressing steel

ϕ understrength factor

ϕ curvature

ϕ_{cr} cracking curvature

ω = $\rho f_y/f'_c$

ω' = $\rho' f_y/f'_c$

ω_p = $\rho_p f_{ps}/f'_c$

$\omega_w, \omega_{pw}, \omega'_w$ reinforcement indices for flanged sections computed as for $\omega, \omega_p, \omega'$ except that b is the web width, and the steel area is that required to develop the compressive strength of the web only.

Units

The Monte Carlo study was carried out using the basic units of pounds and inches. Thus, the forces were in pounds, the dimensions were in inches, the stress was in psi, and the moment was in in-lbs.